発表者氏名	論文タイトル名	発表誌名	巻号	ページ	出版年
Deng, L., Shoji, I., Ogawa, W., Kaneda, S., **Soga, T.,** Jiang, D., Ide, Y., Hotta, H.	"Hepatitis C Virus Infection Promotes Hepatic Gluconeogenesis through an NS5A-Mediated, FoxO1-Dependent Pathway"	J. Virol.	85(17)	8556-8568	2011
Hayashi, K., Sasamura, H., Hishiki, T., Suematsu, M., Ikeda, S., **Soga, T.,** Itoh, H.	"Use of Serum and Urine Metabolome Analysis for the Detection of Metabolic Changes in Patients with Stage 1-2 Chronic Kidney Disease"	Nephro-Urol. Mon.	3(3)	164-171	2011
Kato, T., Niizuma, S., Inuzuka, Y., Kawashima, T., Okuda, J., Kawamoto, A., Tamai, Y., Iwanaga, Y., **Soga, T.,** Kita, T., Kimura, T., Shioi, T.	"Analysis of Liver Metabolism in a Rat Model of Heart Failure"	Int. J. Cardiol.	online	doi:10.1016/j.ijcard.2011.07.056	2011
Suzuki, T., Toyohara, T., Akiyama, Y., Takeuchi, Y., Mishima, E., Suzuki, C., Ito, S., **Soga, T.,** Abe, T.	"Transcriptional Regulation of Organic Anion Transporting Polypeptide SLCO4C1 as a New Therapeutic Modality to Prevent Chronic Kidney Disease"	J. Pharm. Sci.	100(9)	3696-3707	2011
Sugimoto, M., Sakagami, H., Yokote, Y., Onuma, H., Kaneko, M., Mori, M., Sakaguchi, Y., **Soga, T.,** Tomita, M.	"Non-targeted metabolite profiling in activated macrophage secretion "	Metabolomics	online	DOI: 10.1007/s11306-011-0353-9	2011
平山明由、曽我朋義	CE-MSメタボローム測定法	Diabetes Frontier	Vol.22, No.6	pp673-678	2011
曽我朋義	新規酸化ストレスマーカーγ-グルタミルジペプチドによる肝疾患スクリーニング	酸化ストレスと肝疾患	第7巻	pp115-123	2011

1521-009X/12/4001-169–177$25.00
DRUG METABOLISM AND DISPOSITION
Copyright © 2012 by The American Society for Pharmacology and Experimental Therapeutics
DMD 40:169–177, 2012

Vol. 40, No. 1
41137/3740016

Acetaminophen-Induced Hepatotoxicity in a Liver Tissue Model Consisting of Primary Hepatocytes Assembling around an Endothelial Cell Network

Yu Toyoda, Miho Tamai, Kasumi Kashikura, Shunsuke Kobayashi, Yoichi Fujiyama, Tomoyoshi Soga, and Yoh-ichi Tagawa

Department of Biomolecular Engineering, Graduate School of Bioscience and Biotechnology, Tokyo Institute of Technology, Yokohama, Japan (Y.To., M.T., S.K., Y.Ta.); Institute for Advanced Biosciences Keio University, Yamagata, Japan (K.K., T.S.); and Optical Components Consumer & Optical Products Department Shimadzu, Corporation, Kyoto, Japan (Y.F.)

Received June 10, 2011; accepted October 18, 2011

ABSTRACT:

Primary hepatocytes have been used in drug development for the evaluation of hepatotoxicity of candidate compounds. However, the rapid depression of their hepatic characters in vitro must be improved to predict toxicity with higher accuracy. We have hypothesized that a well organized tissue construct that includes nonparenchymal cells and appropriate scaffold material(s) could overcome this difficulty by remediating the viability and physiological function of primary hepatocytes. In this study, we constructed an in vitro liver tissue model, consisting of mouse primary hepatocytes assembling around an endothelial cell network on Engelbreth-Holm-Swarm gel, and examined its response to acetaminophen treatment. The increase in lactate dehydrogenase release after the exposure to acetaminophen was induced earlier in the liver tissue model than in monolayer hepatocytes alone, suggesting that the tissue model was more sensitive to an acetaminophen-induced toxicity. On the basis of our results, we conclude that liver tissue models of this kind may enhance the responses of hepatocytes against xenobiotics via the maintenance of hepatic genes and functions such as cytochrome P450s. These findings will contribute to the development of more accurate systems for evaluating hepatotoxicity.

Introduction

Despite the dramatic and evolutional progress made in life sciences over the last decade, the productivity of pharmaceutical companies in bringing new drugs to the market has not been improved (Kola and Landis, 2004; Paul et al., 2010). Nonetheless, research and development expenditure has been increasing, and the high rate of candidate attrition during development has been a considerable problem. To address these issues, a great deal of effort has been devoted toward reducing the candidate attrition in the late stages of drug development, as well as toward producing new drugs more cost effectively (Gleeson et al., 2011; Kwong et al., 2011). It is important to predict and/or detect the toxicity of the drug candidates as early as possible during the process of drug development.

The liver is a multifunctional organ involved in the metabolism, detoxification, and excretion of substances. Therefore, compound-induced hepatotoxicity is a major issue in drug discovery and development (Jaeschke et al., 2002; Kaplowitz, 2005). Although many in vitro trials have used primary cultured hepatocytes prepared from the liver, these cells pose several problems for in vitro hepatotoxicity assays. When cultured by themselves, hepatocytes cannot continue to grow or maintain their specific functions in vitro. The liver is composed of not only parenchymal hepatocytes but also nonparenchymal cells, such as sinusoidal endothelial cells, Kupffer cells, and others. Hepatocytes can express their specific functions only in the structural environment of hepatic tissue. To make it possible for primary hepatocytes to survive for long periods and maintain their specific functions in vitro, it is important to maintain cell-cell interactions, both between hepatocytes and between hepatocytes and nonparenchymal cells (Bhatia et al., 1998, 1999; Strain, 1999; Kidambi et al., 2009), as

This work was supported by the Precursory Research for Embryonic Science and Technology and the Adaptable and Seamless Technology transfer Program through target-driven R&D funding [Grant AS2211513G] from the Japan Science and Technology Agency (JST); a Grant-in-Aid for Scientific Research (B) [Grant 21300178] from the Japanese Society for the Promotion of Science (JSPS); and a Grant-in-Aid for Scientific Research on Innovative Areas [Grant 23119003] from the Ministry of Education, Culture, Sports, Science and Technology. Y.To. and M.T. are JSPS research fellows.

Article, publication date, and citation information can be found at http://dmd.aspetjournals.org.

http://dx.doi.org/10.1124/dmd.111.041137.

ABBREVIATIONS: ECM, extracellular matrix; ES, embryonic stem; IVL^{mES}, mouse ES cell-derived in vitro liver tissue model; HUVEC, human umbilical vein endothelial cell; NAPQI, *N*-acetyl-*p*-benzoquinone imine; IVL, in vitro liver model; APAP, *N*-(4-hydroxyphenyl)acetamide; EHS, Engelbreth-Holm-Swarm; OHT, hydroxytestosterone; HP, hydroxyprogesterone; EGM-2, endothelial cell growth medium-2; DMEM, Dulbecco's modified Eagle's medium; HBSS, Hank's balanced salt solution; LDH, lactate dehydrogenase; HPLC, high-performance liquid chromatography; CE-TOFMS, capillary electrophoresis coupled with electrospray ionization time-of-flight mass spectrometry; PECAM-1, platelet endothelial cell adhesion molecule-1; vWF, Von Willebrand factor; HGF, hepatocyte growth factor; IVL$_{EHS}$, in vitro liver model on EHS gel; RT-PCR, reverse transcription-polymerase chain reaction; hprt, hypoxanthine-guanine phosphoribosyltransferase; TAT, tyrosine aminotransferase.

well as proper extracellular matrix (ECM) (Kleinman et al., 2003; Takashi et al., 2007).

In this context, we have focused on the interaction between hepatocytes and endothelial cells. In 2005, we successfully achieved hepatic organogenesis from murine embryonic stem (ES) cells (Ogawa et al., 2005; Tsutui et al., 2006). This mouse ES cell-derived in vitro liver tissue model (IVL^{mES}) included both hepatocyte layers and a sinusoid vascular network; the model was capable of recapitulating most hepatic functions. Due to imperfect control of the hepatic regions in IVL^{mES}, it was difficult to quantitatively evaluate metabolites in this system. However, Nahmias et al. (2006) reported a culture system, "liver-like tissue" that included fewer components. Their system consists of two types of cells, primary hepatocytes and an endothelial cell network that formed vascular structures. As with IVL^{mES}, liver-like tissue exhibited long-term expression of hepatic genes such as albumin. It would be reasonable to expect that an optimized liver-like tissue would be a useful system for evaluating the hepatotoxic potential of candidate drug compounds.

In this study, we used both mouse primary hepatocytes and human umbilical vein endothelial cells (HUVECs), a representative type of endothelial cells, to construct an in vitro liver model (IVL) for use in drug screening. Using these two types of cells allowed us to specifically examine the expression of hepatic genes and resulted in development of a simple, cost-effective system. Next, we investigated the response of IVL to xenobiotic treatment to assess the utility of this system in the evaluation of hepatotoxicity.

Acetaminophen [APAP; *N*-(4-hydroxyphenyl)acetamide; $C_8H_9NO_2$] is one of the most commonly used drugs for the treatment of pain and fever; its reactive metabolite, *N*-acetyl-*p*-benzoquinone imine (NAPQI), oxidized by cytochrome P450 isozymes such as CYP2E1, causes hepatocyte damage (Hayes and Pickering, 1985; Lee et al., 1996; Jaeschke et al., 2003; James et al., 2003). Compared with an in vivo acute liver injury model, in vitro trials using monolayer-cultured hepatocytes generally requires more time for the definite observation APAP cytotoxicity. We have hypothesized that the gap between in vivo and in vitro hepatic reactions could be filled using a well organized tissue construct that included nonparenchymal cells and appropriate scaffold matrix to improve the viability and physiological function of hepatocytes.

To verify this hypothesis, we have constructed an in vitro liver tissue model and examined its response to APAP treatment. In short-term culture, our liver tissue model was more sensitive to APAP-induced toxicity than were hepatocytes alone. Our results suggest that the presence of endothelial cells enhances the responsiveness of hepatocytes to xenobiotics.

Materials and Methods

Cells and Materials. HUVECs were obtained from Cambrex BioScience Walkersville, Inc. (Walkersville, MD). EBM-2 (endothelial cell basal medium) and EGM-2 Single Quots (supplemental factors) were purchased from Lonza Japan Ltd. (Tokyo, Japan). Dulbecco's modified Eagle's medium (DMEM), penicillin/streptomycin (100×), and trypsin-EDTA were from Invitrogen (Carlsbad, CA). Tissue-culture treated cell culture dishes/plates were acquired from Corning Inc. (Tokyo, Japan). Collagenase, trypsin inhibitor, mannitol, D-camphor-10-sulfonic acid, 1,3,5-benzenetricarboxylic acid (trimesate) and gelatin were purchased from Wako Pure Chemical Industries, Ltd. (Osaka, Japan). 2-(*N*-morpholino)ethanesulfonic acid was obtained from Dojindo Laboratories (Kumamoto, Japan). Laminin, fibronectin, poly-D-lysine, collagen type I, collagen type IV, and growth factor-reduced Engelbreth-Holm-Swarm (EHS) gel were purchased from BD Biosciences (Bedford, MA), and stored at −30°C until use. Acetaminophen (*p*-acetamidophenol) was purchased from Nacalai Tesque, Inc. (Kyoto, Japan). Testosterone (4-androsten-17β-ol-3-one), 6β-hydroxytestosterone (OHT), 2α-OHT, and 11α-hydroxyprogesterone (HP) were purchased from Sigma-Aldrich (St. Louis, MO). 16α-OHT, 16β-OHT, and 7α-OHT were purchased from Daiichi Pure Chemicals Corp. (Tokyo, Japan). 3-(*N*-acetyl-L-cysteine-*S*-yl)acetaminophen (acetaminophen mercapturate) was obtained from Santa Cruz Biotechnology, Inc. (Santa Cruz, CA). All reagents used were of analytical grade.

Animals. Male, 6- to 10-week-old BALB/cAJcl mice were purchased from CLEA Japan Inc. (Tokyo, Japan) and were treated in accordance with local institutional guidelines for the care and use of laboratory animals. DsRed2 transgenic mice carrying the expression vector of DsRed2 fluorescence protein gene, controlled by the CAG promoter, were originally obtained via a DsRed2-expressing ES cell-contributing chimera mouse produced by the aggregation chimera method. The F_1 offspring expressing DsRed2 protein has been backcrossed with BALB/cAJcl mice finally to 20 generations. DsRed2 BALB/cAJcl transgenic mice (male, 6-week-old) were used in this study for DsRed2 fluorescent assay. The animal protocol was approved by the Animal Experimentation Committees of Tokyo Institute of Technology.

Preparation of Cell Culture Substrate. Gelatin-coated surfaces were prepared by incubation with heat-sterilized 0.05% gelatin solution for 3 h at 4°C. Thawing EHS gel was poured into ice-cold 6-well plates (500 μl/wells) and incubated for 30 min at 37°C to allow polymerization. Laminin, fibronectin, poly-D-lysine, collagen type I, and collagen type IV (50 μg protein/well) were coated onto surfaces according to the manufacturer's instructions.

Cell Culture. HUVECs were maintained in complete EGM-2 [EBM-2 with instructed supplementations as follows: 2% (v/v) fetal bovine serum, hydrocortisone, human fibroblast growth factor-β, vascular endothelial growth factor, R3-IGF-1, ascorbic acid, human epidermal growth factor, GA-1000 (Gentamicin, Amphotericin-B), and heparin] at 37°C in a humidified atmosphere of 5% CO_2 in air. The passage of cells was limited to 10 times. Isolated hepatocytes were maintained in DMEM supplemented with 100 U/ml penicillin and 100 μg/ml streptomycin at 37°C in a humidified atmosphere of 5% CO_2 in air.

Isolation of Primary Hepatocytes from Mouse Liver. Hepatocytes were prepared from mice anesthetized with pentobarbital by an in situ 2-step collagenase perfusion method (Seglen, 1976), with slight modifications. In brief, after the cannulation of isolated portal vein with a 24-gauge catheter (Terumo, Tokyo, Japan), mouse liver was preperfused in situ with Hank's balanced salt solution (HBSS) containing EGTA (0.19 g/l) and glucose (0.98 g/l) to remove the blood; next, the liver was perfused with 0.015% collagenase in HBSS. After the extraction of the liver, the cells were dispersed in ice-cold HBSS (pH 7.2) by blade mincing. The cells obtained were filtered through a 100-μm pore mesh nylon cell strainer (BD Biosciences) and centrifuged twice for 2 min at 500*g* to remove nonparenchymal cells. Subsequently, for further purification, the remaining cells were centrifuged for 2 min at 1200*g* and then subjected to 40% Percoll density gradient centrifugation for 10 min at 1200*g*. At this stage, cell viability measured by the trypan blue method was >85%. The isolated hepatocytes were plated at a cell density of 1.0×10^6 cells per well in 6-well plates; cells were grown in DMEM containing 10% (v/v) heat-inactivated fetal bovine serum, 100 U/ml penicillin, and 100 μg/ml streptomycin at 37°C in a humidified incubator with 5% CO_2/95% air. The medium for cell attachment was replaced with fresh medium after the first 4 h of incubation. One day later, the growth medium was exchanged with serum-free medium, and replaced daily thereafter.

Detection of mRNA by Reverse Transcription-Polymerase Chain Reaction. Total RNA was isolated using the acid guanidinium-phenol-chloroform method according to a standard protocol described elsewhere. The purity and concentrations of isolated RNA were assessed by absorbance determination, and the integrity of the RNA was verified by 0.6% agarose gel electrophoresis in TAE buffer (20 mM Tris acetate, 0.5 mM EDTA, pH 8.0). First-strand cDNA was prepared from the extracted total RNA in a reverse-transcriptase reaction, using the SuperScript II Reverse Transcriptase kit and oligo(dT) primer (Invitrogen) according to the manufacturer's instruction. The cDNA from mRNA of the genes of interest were amplified by PCR in a GeneAmp PCR System 9700 thermal cycler (Applied Biosystems, Foster City, CA) with a set of specific primers (Tables 1 and 2). After the PCR, the resulting amplicons were separated by 1.5% (w/v) agarose gel electrophoresis with TBE buffer (44.5 mM Tris, 44.5 mM boric acid, 10 mM EDTA, pH 8.0) and detected with ethidium bromide under UV light.

Urea Assay. Culture medium collected in each measurement period was centrifuged for 5 min at 300*g* to remove floating cells, and supernatant was

TABLE 1

Primer information for human gene

Gene	GenBank Accession Number	Sequences (5′>3′)	Position	Product
				bp
PECAM1	NM_000442	F: ACGGAATCCTTCTCTACACC	901–920	477
		R: TGCAGTGCAGATATACGTCC	1377–1358	
vWF	NM_000552	F: TGCAACACTTGTGTCTGTCG	2786–2805	486
		R: TGCAGTGCAGATATACGTCC	3271–3251	
HGF	NM_000601	F: CCGAACAGGATTCTTTCACC	101–120	372
		R: TATTGAAGGGGAACCAGAGG	472–453	
GAPDH	NM_002046	F: AGATCATCAGCAATGCCTCC	536–555	492
		R: TGACAAAGTGGTCGTTGAGG	1027–1008	

F, forward; r, reverse; bp, base pairs.

stored at −80°C until determination of urea levels. Urea was detected in culture medium using a QuantiChrom Urea Assay Kit (BioAssay Systems, Hayward, CA). In brief, 5 μl of the obtained solvent was incubated with a 200-μl reaction mixture for 30 min at room temperature. The urea-dependent chromogenic reaction was read using an iMark Microplate Reader (Bio-Rad Laboratories, Hercules, CA) at 492 nm. To calculate the urea concentration of each sample, known concentrations of urea were used to generate a standard curve.

WST-1 Assay. The viability of cells was evaluated using a Cell Counting Kit (Dojindo Laboratories). In brief, cells were seeded in 96-well plates (4×10^4 cells/well) and cultured at 37°C for 24 h. Acetaminophen was added to the culture medium at various concentrations, and incubation was continued for an additional 24 h. Subsequently, the culture medium was replaced with 110 μl of fresh medium containing 10% (v/v) of the WST-1 assay reaction mixture. Cells were again incubated for 90 min, and 100 μl of the resulting supernatant was transferred to a 96-well microplate. The reduction of WST-1 was measured photometrically using an iMark Microplate Reader at 450 nm.

Lactate Dehydrogenase Assay. After incubation for the indicated periods, the culture medium was collected and centrifuged for 5 min at 300*g*, and the supernatant was used for determination of lactate dehydrogenase (LDH) level in the culture medium. To detect the LDH levels in whole-cell lysate, the remaining cells were treated with 10 mM phosphate buffer (pH.7.4) containing 1% (w/v) Triton X-100. The cell suspension sample containing the dissolved scaffold materials was homogenized by passage through a 27-gauge needle and then centrifuged for 10 min at 800*g* at 4°C. The resulting supernatant fraction (whole-cell lysate) was transferred to a new tube. LDH levels in each fraction (culture medium and whole-cell lysate) were detected using SPOTCHEM EZ SP-4430 and SPOTCHEM II LDH (ARKRAY, Kyoto, Japan). Media-released LDH ratio (percentage) was calculated using the following formula: media-released LDH ratio (%) = $LDH_{media}/(LDH_{media} + LDH_{whole\text{-}cell\ lysate}) \times 100$.

Fluorescence Intensity Assay. To count the amount of living hepatocytes quantitatively, DsRed2 fluorescence intensity was measured 24 h after the seeding of red hepatocytes isolated from the DsRed-transgenic mouse. The DsRed2 fluorescence derived from the living red-fluorescent hepatocytes attaching on the culture surface was measured by using LAS-4000 system (Fujifilm, Tokyo, Japan). Obtained images were analyzed by Multi Gauge program, version 3.1 (Fujifilm).

Testosterone Metabolism Assay. To examine the enzymatic activities of cytochrome P450s, each metabolite of testosterone in the culture medium was quantitatively detected using high-performance liquid chromatography (HPLC) as described previously (Tsutui et al., 2006) with some modification. In brief, testosterone and its metabolites were separated using an HPLC system (LC-10AD VP; Shimadzu, Kyoto, Japan) equipped with a reversed-phase C18 column (Cadenza CD-C18, 10 mm × 250 mm; Tosoh, Tokyo, Japan) maintained at 40°C. Elution solvents were as follows: solvent A (water/methanol/acetonitrile: 39:60:1 v/v) and solvent B (water/methanol/acetonitrile: 80:18:2 v/v). Elution was started with 18% solvent B and 82% solvent A for 10 min, followed by elution with a linear gradient of solvent B (18–80%) for the next 10 min. Afterward, 80% solvent B was maintained for 30 min. The elution flow throughout was kept constant at a rate of 0.5 ml/min, and testosterones were detected by UV absorbance at 254 nm. The resulting chromatograms were analyzed using the LC Solutions software (Shimadzu). The peak of each metabolite was compared with that of the internal standard to determine its quantity. To obtain the standard chromatogram, 2α-OHT, 6β-OHT, 7α-OHT, 11α-HP, 16α-OHT, and 16β-OHT were subjected to independent analyses.

CE-TOFMS Analysis. 3-(*N*-acetyl-L-cysteine-*S*-yl)acetaminophen, one of the APAP metabolites, was detected using the CE-TOFMS method as described previously (Soga et al., 2006). In brief, after the 5% mannitol treatment, cells on the EHS gel were saturated with 1 ml of MeOH containing 25 μM of each internal standard (methionine sulfate, 2-(*N*-morpholino)ethanesul-

TABLE 2

Primer information for mouse gene

Gene	GenBank Accession Number	Sequences (5′>3′)	Position	Product
				bp
Albumin	NM_009654	F: GCTACGGCACAGTGCTTG	1224–1241	266
		R: CAGGATTGCAGACAGATAGTC	1489–1469	
Tat	NM_146214	F: CAATCCTGGACAGAACATCC	565–584	280
		R: GATCTCATCGGCTAAGATGG	844–825	
Cyp1a2	NM_009993	F: GTCACCTCAGGGAATGCAGTGG	744–765	493
		R: AGGTGTCCCTCGTTGTGCTGTG	1236–1215	
Cyp2e1	NM_021282	F: TGTGACTTTGGCCGACCTGTTC	889–910	446
		R: CAACACACACGCGCTTTCCTGC	1334–1313	
Cyp2r1	NM_000442	F: CGGAAGATGCAGTTGTACGTGGC	1166–1188	477
		R: TCTGCACAGATGAGGTAGGGCTG	1511–1489	
Cyp3a	NM_007818	F: AATTCCTGGGCCCAAACCTCTGC	189–211	496
		R: AGGATCCTCTGGGTTGTTGAGGG	684–662	
Abcb11	NM_021022	F: TGGCCAGATCACCAACGAAGCC	2935–2956	513
		R: TGCCCAGGATCCACAGATACCG	3447–3426	
Abcc2	NM_013806	F: TGTGGATAATGAGGCGCCGTGG	3921–3942	452
		R: TGGAGCAACCCAAGTTGCAGGC	4373–4352	
Hprt	NM_013556	F: GTAATGATCAGTCAACGGGG	463–482	441
		R: AGCTTTACTAGGCAGATGGC	903–884	

F, forward; r, reverse; bp, base pairs.

fonic acid, and D-camphor-10-sulfonic acid) for 10 min to extract the metabolites. The resulting solution was immediately mixed with 400 μl of $CHCl_3$ and 200 μl of water and centrifuged at 10,000g for 3 min at 4°C. Subsequently, the 400-μl upper aqueous layer was centrifugally filtered through a Millipore 5-kDa cutoff filter (Millipore Corporation, Billerica, MA) to remove proteins. The filtrate was lyophilized and dissolved in 50 μl of MilliQ water containing reference compounds (3-aminopyrrolidine and trimesate) before CE-TOFMS analysis.

CE-TOFMS analysis was performed using an Agilent CE capillary electrophoresis system (Agilent Technologies, Waldbronn, Germany), an Agilent G3250AA LC/MSD TOF system (Agilent Technologies, Palo Alto, CA), an Agilent1100 series binary HPLC pump, a G1603A Agilent CE-MS adapter, and a G1607A Agilent CE-ESI-MS sprayer kit. For system control and data acquisition, we used the G2201AA Agilent ChemStation software for CE and the Analyst QS software for TOFMS. CE-TOFMS analysis for anionic metabolites was carried out according to a previous report (Soga et al., 2009).

Statistical Tests. Experimental data were expressed as means ± S.D. and analyzed by determining the statistical significance according to Student's t test. Differences were considered significant when $P < 0.05$.

Results

Establishment and Characterization of the In Vitro Liver Tissue Model on EHS Gel. HUVECs, a representative type of endothelial cells, were seeded on several scaffold materials (gelatin, laminin, fibronectin, poly-D-lysine, collagen type I, collagen type IV, or EHS gel), to investigate what kind of scaffold material is useful for inducing the functions of endothelial cell. As shown in Fig. 1A, HUVECs grew with normal spreading and displayed a cobblestone morphology within 24 h when grown on laminin, fibronectin, poly-D-lysine, collagen type I, or collagen type IV, as well as on gelatin-coated or noncoated tissue culture 6-well plates. However, on EHS gel, HUVECs rapidly elongated and generated a network structure (Fig. 1A). After the seeding of HUVECs (3.5×10^5 cell/well in 6-well plates), network morphogenesis on EHS gel was accomplished within a few hours and could be maintained for at least 4 days (Fig. 1B). Subsequently, to compare the maintenance of endothelial cell character of HUVECs on each scaffold material, we measured the expression of endothelial cell-specific marker genes, such as *platelet endothelial cell adhesion molecule-1* (*PECAM-1*) and *Von Willebrand factor* (*vWF*) (Fig. 1C). In HUVECs cultured on EHS gel, expression of these genes was maintained at a high level compared with cells grown on other scaffold materials. It is noteworthy that hepatocyte growth factor (HGF) was strongly expressed in HUVECs only on EHS gel (Fig. 1C).

On this network structure of HUVECs, freshly isolated mouse primary hepatocytes (1.0×10^6 cell/well in 6-well plates) were seeded and cultured. The primary hepatocytes migrated toward the HUVEC network and piled next to one another within 24 h, forming a structure that resembled hepatic tissue (Fig. 1, D and E). This structure could be maintained for 5 days, at least until the disruption of HUVEC network. In the absence of a HUVEC network, primary hepatocytes seeded on EHS gel almost never aggregated with each other. The presence of HUVEC on gelatin did not affect the cobblestone morphology of hepatocytes (Fig. 1D). According to the scheme described in Fig. 1F, this in vitro liver tissue model on EHS gel, which we term IVL_{EHS}, was used in the following experiments.

To confirm whether there was no difference in the percentage of attachment of hepatocytes between gelatin and EHS gel, we used red-fluorescent hepatocytes from the livers of DsRed2-transgenic mice. Based on the linear relationship between the signal intensity of DsRed2 fluorescence and the total amount of red hepatocytes (Fig. 1G), the number of hepatocytes finally attaching on the surface of each culture conditions was almost the same (Fig. 1H).

The IVL_{EHS} Could Maintain Its Hepatic Function for a Longer Period than Monolayer Culture of Hepatocytes. To compare the effect of the IVL_{EHS} to general primary hepatocyte culture on gelatin, we investigated the level of urea production, a major hepatic function (Fig. 2). After the first 24 h, urea production did not differ between samples, regardless of whether primary hepatocytes were cocultured with HUVECs or whether they were grown on gelatin or EHS gel; however, urea levels in the culture were lower when the cells were grown on EHS gel than on gelatin (Fig. 2A). The urea level in the culture medium of the HUVEC network alone was too low (less than several hundred micrograms per deciliter) to recognize a significant effect (data not shown). To estimate the ratio of decrease in relative urea levels on EHS gel (Fig. 2A), identical volumes (2.0 ml) of urea

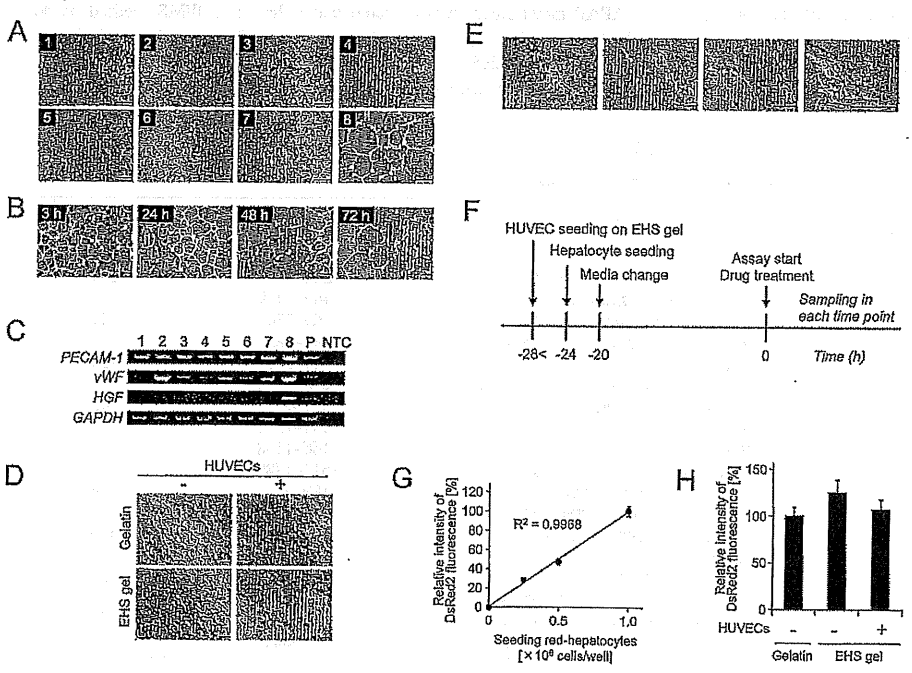

FIG. 1. Characterizations of the IVL_{EHS}. A, microscopic images of HUVECs on each scaffold material after 24 h of culture. 1, tissue-culture treated; 2, gelatin; 3, laminin; 4, fibronectin; 5, poly-D-lysine; 6, collagen type I; 7, collagen type IV; 8, growth factor-reduced EHS gel. B, time-dependent construction of the HUVEC network on EHS gel soon after seeding. C, RT-PCR analysis of HUVECs on each scaffold material: lane 1, tissue-culture treated; 2, gelatin; 3, laminin; 4, fibronectin; 5, poly-D-lysine; 6, collagen type I; 7, collagen type IV; 8, growth factor-reduced EHS gel; P, positive control (cDNA library of human adult liver); NTC, nontemplate control; glyceraldehyde-3-phosphate dehydrogenase (GAPDH), internal loading control. D and E, microscopic images of the in vitro liver tissue model consisting of primary hepatocytes and HUVEC network on EHS gel. All images were obtained 24 h after the seeding of hepatocytes. F, schemes for construction and use of IVL_{EHS}. G, the linear relationship between the signal intensity of DsRed2 fluorescence and the total amount of red hepatocytes on gelatin after 24 h of culture. H, the intensity of DsRed2 fluorescence derived from the red hepatocytes in each culture condition. Fluorescence images were obtained 24 h after the seeding of primary red hepatocytes (1.0×10^6 cells per well in 6-well plates) and then analyzed by Multi Gauge program. Data are expressed as the means ± S.E.M. Bars, 500 μm (A and B), 100 μm (D), and 200 μm (E).

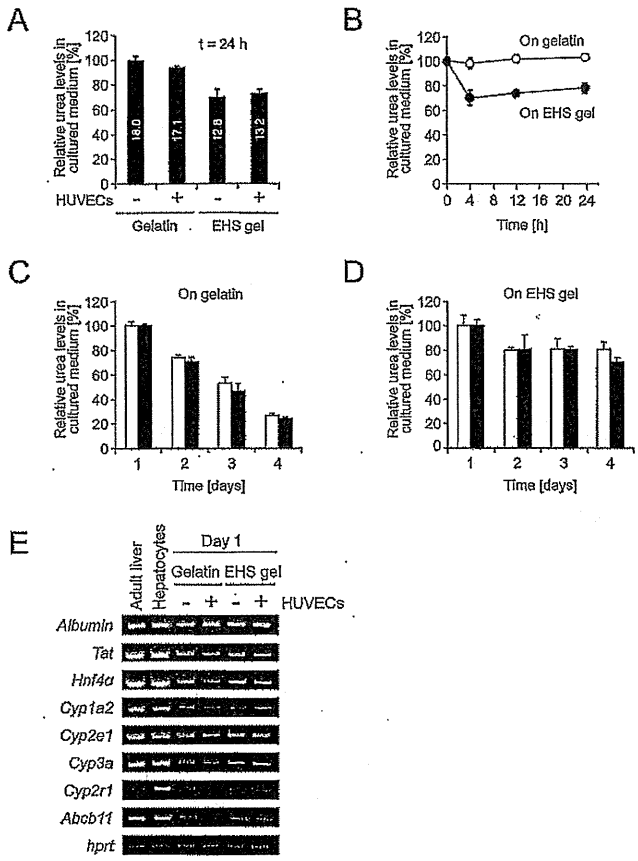

FIG. 2. Validation of hepatic function in IVL_{EHS}. A, urea levels in the culture medium in each culture condition, at 24 h. Data are calculated as ratios by referring to the urea level of hepatocyte monolayers cultured on gelatin. B, apparent decrease in urea level in culture medium incubated on EHS gel. Identical volumes of urea-containing precultured medium were incubated on gelatin or EHS gel. C and D, time-dependent change of urea productivity of hepatocyte with (closed columns) or without (open columns) HUVECs on gelatin (C) or EHS gel (D). Culture medium was changed every day over the course of the measurement period. Data are calculated as ratios by referring to the urea level on day 1 in each culture condition. Data are expressed as the means ± S.D. of triplicate determinations. E, expression levels of hepatic genes. Adult liver, mouse adult liver at 8 weeks of age; Hepatocytes, hepatocytes immediately after isolation; hprt, internal loading control.

containing precultured medium were incubated on gelatin and EHS gel. As shown in Fig. 2B, a decrease in the urea level was observed on EHS gel in the absence of primary hepatocytes, suggesting that ~30% of the urea was absorbed by the EHS gel. The urea productivity of hepatocytes was not affected by the type of scaffold material or the existence of HUVECs (Fig. 2, A and B).

To investigate whether IVL_{EHS} is superior to other models with regard to the maintenance of liver-specific functions, we examined the time-dependent change of urea productivity during the period when the HUVEC network was adequately maintained. In the case of monolayer culture on gelatin, the urea productivity of hepatocytes rapidly decreased each day (Fig. 2C). In contrast, culture on EHS gel made the cells comparatively resistant to this decrease (Fig. 2D). Although the presence of HUVECs did not enhance the potential urea productivity of hepatocytes, EHS gel was superior to gelatin with respect to the maintenance of hepatic functions.

To investigate any possible change in the hepatic gene expression, hepatocytes were cultured in each condition with or without HUVECs for 24 h and subjected to reverse transcription-polymerase chain reaction (RT-PCR) analysis. IVL_{EHS} also retained some cytochrome P450 expression at least, as well as monolayer cultured hepatocytes (Fig. 2E), suggesting that the hepatic potential of IVL_{EHS} was not lower than that of monolayer cultured hepatocytes.

Measurement of In Vitro Hepatotoxicity Induced by Acetaminophen Treatment. We next examined the hepatotoxicity in the liver tissue model induced by APAP; this treatment was intended to simulate an exogenous stimulus triggered by xenobiotic treatment. At first, to evaluate the effect of APAP on the cytotoxicity of hepatocytes, we incubated hepatocytes on gelatin with APAP at different concentrations for 36 h. Hepatocyte viability was measured by the WST-1 assay. Because 10 mM APAP was sufficient to induce hepatocyte death within 36 h (Fig. 3A), we chose 10 mM APAP as the direct toxicant concentration for the following experiments. The release of LDH into the cultured medium was measured at various time points. Differences between APAP-treated and untreated samples started to be observed 24 h after the addition of APAP (Fig. 3B). After 36-h exposure to APAP, LDH level in the culture medium of treated cells was significantly higher than in the control (Fig. 3B). Microscopic observation indicates that the monolayer-cultured hepatocytes were lethally injured, and that the normal cytoplasmic projections of spreading hepatocytes, present in control culture on gelatin, were disrupted (Fig. 3C). The hepatocytes cultured on EHS gel were also injured. The architecture of the liver tissue model, with hepatocytes massing around the HUVEC network, maintained its appearance (Fig. 3C). It is noteworthy that exposure to APAP for 36 h did not affect the final levels of LDH in any culture condition, but it did affect the time-dependent increase of LDH (Fig. 3D).

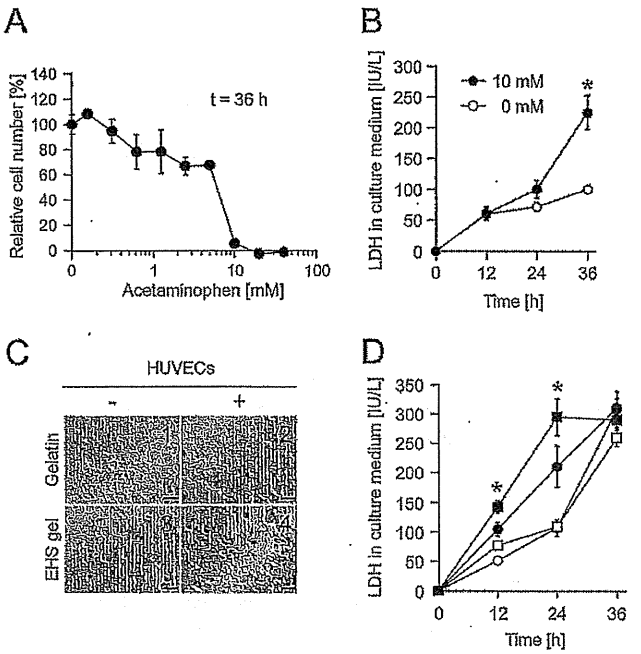

FIG. 3. Measurement of in vitro hepatotoxicity induced by acetaminophen treatment. A, dose-dependent cytotoxicity induced by APAP. Hepatocytes cultured on gelatin were treated with APAP at various concentrations for 36 h. The relative number of hepatocytes was evaluated by WST-1 assay. B, time-dependent change of LDH levels in the culture medium, for hepatocytes on gelatin with (closed circles) or without (open circles) 10 mM APAP. C, microscopic images of hepatocytes in the in vitro liver tissue model (on EHS gel with HUVEC) and other culture conditions (on gelatin with or without HUVEC, and on EHS gel without HUVEC) at 36 h after the APAP treatment. Bars, 50 μm. D, time-dependent increase of LDH in the culture medium upon 10 mM APAP treatment in each culture condition: with (squares) or without (circles) HUVEC; on gelatin (open symbols) or EHS gel (closed symbols). Data are expressed as the means ± S.D. of triplicate determinations. *, significantly different from all other groups ($P < 0.05$).

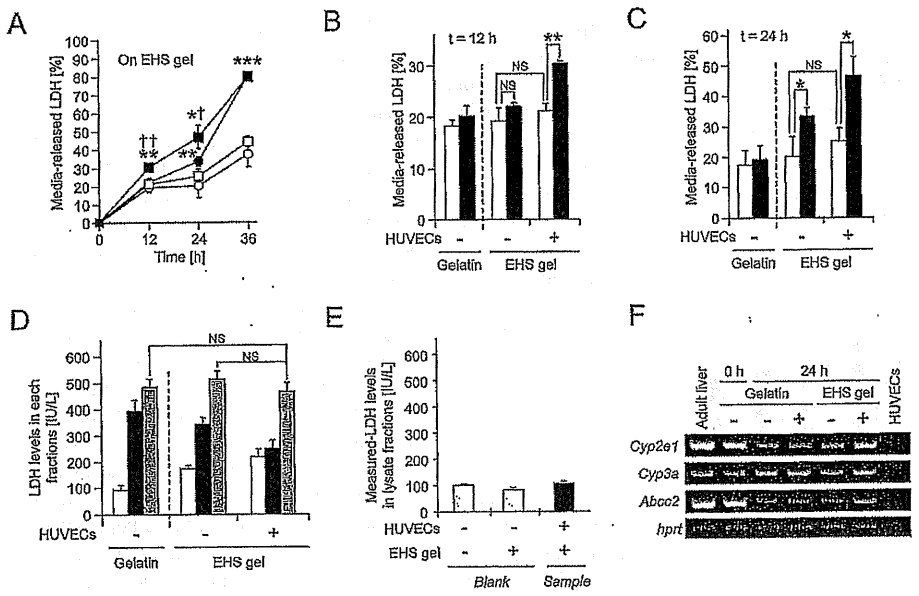

FIG. 4. The effect of construction of the in vitro liver tissue model on APAP-induced hepatotoxicity. A, time-dependent increase of LDH released by hepatocytes on EHS gel in each culture condition, with (squares) or without (circles) HUVEC and with (closed symbols) or without (open symbols) 10 mM APAP. B and C, the ratio of media-released LDH with (closed columns) or without (open columns) 10 mM APAP at 12 (B) and 24 h (C). D, LDH levels in each fraction (cultured medium, open columns; whole-cell lysate, closed columns; total, slashed columns) after 24-h incubation with 10 mM APAP in each culture condition. Data are expressed as the means ± S.D. $n = 3$–9. *, $P < 0.05$; **, $P < 0.01$; ***, $P < 0.001$, relative to the APAP-absent control; †, $P < 0.05$; ††, $P < 0.01$ relative to the HUVEC-absent control; NS, not significant. E, measured-LDH levels in HUVECs cultured on EHS gel after 24 h of culture. Blank (dot) means a non-HUVECs control. These raw data are expressed as the means ± S.D. $n = 3$. F, RT-PCR analysis of hepatocytes cultured with or without HUVECs in each condition. Adult liver, mouse adult liver at 8 weeks of age; hprt, internal loading control.

Enhancement of the Response to Acetaminophen in the IVL_{EHS}. To further investigate whether the construction of the IVL_{EHS} enhances the responsiveness of hepatocytes to APAP, we examined the media-released LDH ratio. As described in Fig. 4A, IVL_{EHS} showed an early response to acetaminophen. Twelve hours after the APAP treatment, the ratio of released LDH in the liver tissue model was already higher than in any controls (Fig. 4B). At this time point, APAP was not directly toxic to HUVECs alone. Hepatocytes alone on EHS gel were also affected by APAP-dependent toxicity after 24 h (Fig. 4C). On the other hand, at those time points, there was no significant difference in the ratio of released LDH caused by APAP treatment in hepatocytes cultured alone on gelatin (Fig. 4, B and C). Furthermore, total LDH levels in hepatocytes incubated with APAP for 24 h were not affected by the type of scaffold material (gelatin or EHS gel) or the presence of HUVECs (Fig. 4D). In this study, the existence of HUVECs had little effect on the LDH level in the culture medium (under the detectable limitation) and whole-cell lysate fraction (Fig. 4E). Under these experimental conditions, HUVECs produced far less LDH than hepatocytes; thus, the increase of LDH release in IVL_{EHS} under the APAP condition appeared to result from the rise of APAP cytotoxicity in hepatocytes. These results suggest that culture on EHS gel could prevent the depression of responsiveness in hepatocytes that is observed in monolayer culture on gelatin; the construction of the IVL_{EHS} would enhance this positive effect further. Finally, to compare the expression level of the *Cyp2e1* gene between IVL_{EHS} and other conditions, RT-PCR analysis was performed 24 h after the seeding of hepatocytes. The expression level of mouse *Cyp2e1* in IVL_{EHS} remained high, compared with other conditions (Fig. 4F). Furthermore, mercapturate, one of the APAP metabolites produced via NAPQI, was quantified by CE-TOFMS in the IVL_{EHS} and primary hepatocyte culture on EHS gel at least 12 h after the APAP treatment. As shown in Table 3, the amount of mercapturate in the IVL_{EHS} was almost the same as that in the primary hepatocyte culture.

Activities of Cytochrome P450 Isozymes in the IVL_{EHS}. The key mechanism underlying APAP hepatotoxicity is cytochrome P450-mediated NAPQI formation (David, 2005). To quantify the P450 activities as major drug-metabolizing enzyme activities in IVL_{EHS}, we quantitatively examined the amount of hydroxylated testosterones in cultured medium. Each P450 enzyme participates independently in the regioselective hydroxylation of testosterone, enabling us to simultaneously investigate the activities of multiple P450s. Testosterone was added into the IVL_{EHS} system, and its metabolites were analyzed by HPLC in their hydroxylated forms. As described in Fig. 5A, retention times of the analytes were as follows: 6β-OHT, 16.3 min; 7α-OHT, 16.9 min; 16α-OHT, 21.3 min; 16β-OHT, 23.9 min; and 2α-OHT, 26.4 min. These products (6β-OHT, 7α-OHT, 16α-OHT, 16β-OHT, and 2α-OHT) were differentially converted by specific cytochrome P450s (Cyp3a, Cyp2a4/5 and 2d9, Cyp2d9 and Cyp2b, Cyp2c29 and Cyp2e, and Cyp2d), respectively. The metabolite profile indicates that activities of P450 isozymes in IVL_{EHS} were higher than those under other conditions (Fig. 5B).

Discussion

Positive Effect of the Construction of IVL_{EHS}. In this study, we showed that culture of hepatocytes in a model that resembles the structure of hepatic tissue is superior to monolayer culture of primary hepatocytes, both in regard to the maintenance of some hepatic genes and the response to xenobiotics, at least in the case of APAP. These findings suggest that this system could be applied to the evaluation of compound-associated hepatotoxicity. Because primary hepatocytes have a more complete set of phase I- and II-metabolizing enzymes than immortalized cell lines, they have been used to develop assay systems that are more representative of in vivo hepatocytes (Dambach et al., 2005). A monolayer system consisting of confluent culture of

TABLE 3

Concentration of 3-(N-acetyl-L-cysteine-S-yl)acetaminophen, mercapturate, in each cellular extraction detected by CE-TOFMS analysis

Data are expressed as the means ± S.D. $n = 3$. There is no significant difference between APAP-treated samples.

HUVEC	APAP Treatment	Mercapturate
		μM/ml extraction
–	–	N.D.
–	+	0.22 ± 0.0414
+	–	N.D.
+	+	0.19 ± 0.0052

N.D., not detected.

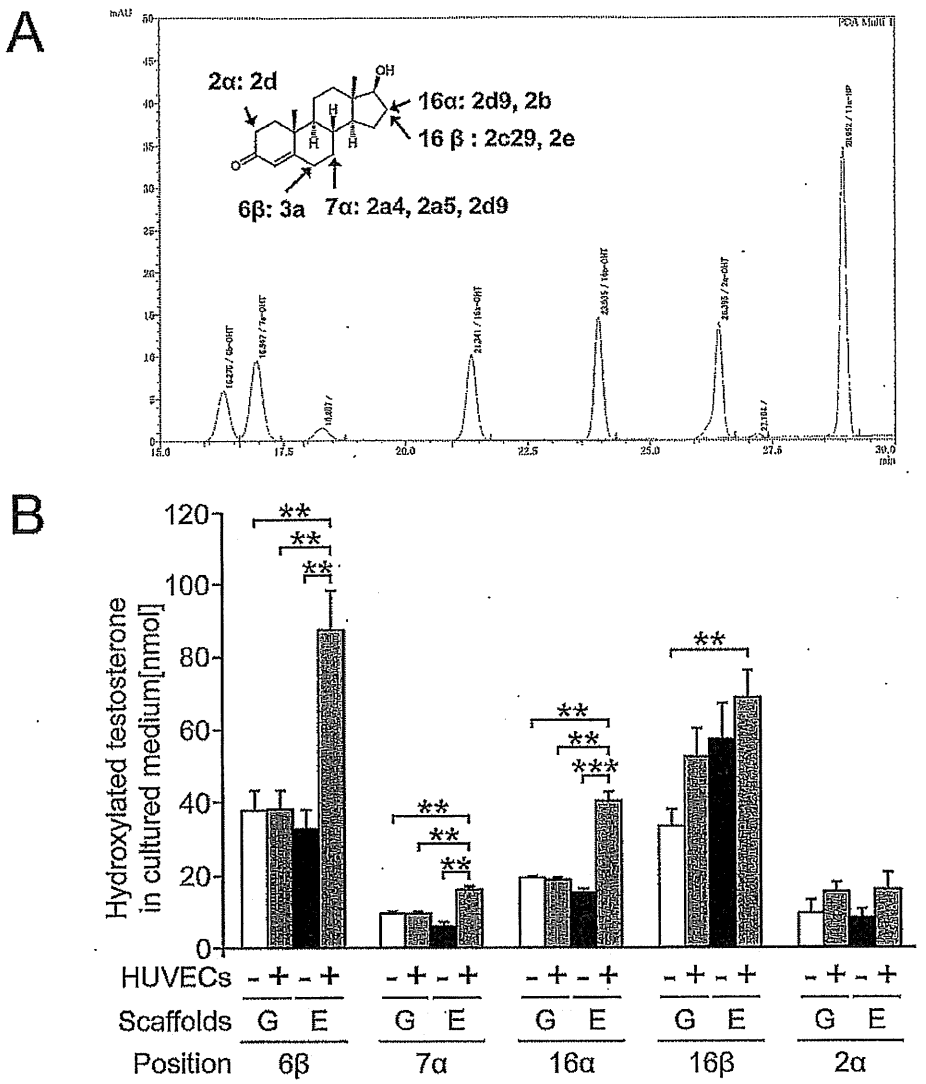

FIG. 5. Testosterone hydroxylation in IVL_{EHS} system. A, HPLC chromatograms of each standard; 6β-OHT (16.3 min), 7α-OHT (16.9 min), 16α-OHT (21.3 min), 16β-OHT (23.9 min), 2α-OHT (26.4 min), and 11α-HP (29 min, as an internal control). B, the amount of each hydroxylated testosterones in culture medium. Data are expressed as the means ± S.D. of triplicate determinations. G, gelatin; E, EHS gel. **, $P < 0.01$; ***, $P < 0.001$.

freshly isolated hepatocytes is already a well established model that provides a better assessment of the metabolic effects and potential hepatotoxicity of interesting compounds (Kikkawa et al., 2006; Hewitt et al., 2007). However, this widely used model has some limitations: low proliferative capacity (not exceeding a few days), loss of liver-specific functions such as drug-metabolizing enzymes, and others. These phenotypic changes reportedly occur early during the isolation process and after seeding, probably as a result of their adaptation to microenvironmental alterations (Guillouzo, 1998). Therefore, we aimed to construct a sophisticated culture condition that mimics the situation in the liver, and examine its utility.

We succeeded in developing a structure that resembles hepatic tissue on EHS gel (Fig. 1). It is well known that the EHS gel induces rapid formation of a capillary-like tubular network of endothelial cells and can preserve hepatocyte functions such as albumin production, expression of some hepatic genes, and others. (Bissell et al., 1987; Kubota et al., 1988). Because EHS gel is an extract of basement membrane proteins derived from the EHS tumor, it consists of various components such as laminin, collagen type IV, proteases such as matrix metallopeptidases, growth factors, and other proteins (Kleinman and Martin, 2005); therefore, in this study, we used growth factor reduced EHS gel to reduce the number of factors that could influence cellular phenotypes. In our examinations, no scaffold material other than EHS gel allowed HUVECs to form networks and generate three-dimensional structures. Further study demonstrated that this cocultivation system of hepatocytes and endothelial cell network was characterized by the expression of HGF, with the HUVEC network functioning as a HGF donor. HGF plays a key role in liver development and maintenance (Schmidt et al., 1995; Matsumoto et al., 2001). Because the active migration of hepatocytes and subsequent adhesion occurred only in the presence of a HUVEC network structure, this phenomenon must be mediated by HGF from HUVEC network. In support of this idea, our research group also found that high levels of soluble HGF protein inhibited hepatocyte migration (Y. Tagawa and S. Kobayashi, unpublished observation). These observations are in agreement with previous reports (Nahmias et al., 2006; Soto-Gutierrez et al., 2010).

Indeed, various factors are able to affect cellular functions of hepatocytes in vitro, and these factors are usually classified into 3 groups, as follows: 1) soluble factors such as cytokines; 2) ECM components that regulate cell behaviors via cell adhesion processes; and 3) cell-cell interactions (Guillouzo et al., 1993). Heterotypic

cell-cell interactions between parenchymal cells and nonparenchymal neighbors play an especially important role in the preservation and modulation of hepatocyte phenotypes in vitro as well as in vivo (Bhatia et al., 1999). As we described under *Results*, the hepatocytes in our in vitro liver tissue model were able to benefit from all three groups of factors: HGF, EHS gel, and hepatocyte-HUVEC interactions correspond to cytokines, ECM, and heterotypic interactions, respectively. Although the specific molecular mechanisms involved in the hepatocyte recruitment process needs to be elucidated, our results suggest the importance of the nonparenchymal cell population for the ex vivo recapitulation of the in vivo liver environment. Further study will shed light on these molecular mechanism(s) and the development of more suitable biomaterials for the construction of in vitro liver tissue models.

Application of IVL_{EHS} to Hepatotoxicity Studies. At present, accumulating evidence suggests that the presence of nonparenchymal cells would be able to support parenchymal cells in vitro as they do in vivo. Nahmias et al. (2006) have reported the endothelium-mediated recruitment of hepatocytes on EHS gel, as well as the stabilization of hepatic function, such as the expression and activity of some *Cyp* genes, in hepatic tissue models that were stable in long-term culture (Soto-Gutierrez et al., 2010). Their experimental evidence supports the future applicability of liver tissue models to the development of bioartificial liver systems. However, their studies were limited to the EHS gel culture and did not include comparison to the gold-standard model. Therefore, we focused on the differences in hepatic functions between our liver tissue model and monolayer culture of hepatocytes.

As shown in Fig. 2, the initial capability of hepatocytes to produce urea depends very little on the culture conditions. However, culture on EHS gel more efficiently preserved hepatic function than culture on gelatin. Under conditions of low external stress, the positive effect of EHS gel is so large that it is difficult to determine the exact contribution of cocultivation with endothelial cells, at least in short-term culture. On the other hand, the construction of a structure resembling hepatic tissue reinforced the responsiveness of hepatocytes to acetaminophen treatment (Figs. 3 and 4).

Acetaminophen is a commonly used analgesic/antipyretic drug, and its overdose induces liver injury in humans and experimental animals. This model hepatotoxicant is converted by a cytochrome P450 enzyme into its reactive metabolite form, NAPQI. In particular, CYP2E1, -1A2, -3A4, and -2A6 play major roles in this oxidation process (James et al., 2003). At therapeutic doses of acetaminophen, the reactive metabolite is efficiently detoxified by glutathione conjugation. However, at a toxic dose, glutathione is depleted by this conjugation, and the excess metabolite covalently binds to protein, resulting in the induction of oxidative stress and the development of toxicity (Jaeschke et al., 2003; James et al., 2003; Reid et al., 2005).

According to in vivo experiments and clinical evidence, these events occur within a few hours after the administration of a toxic dose of acetaminophen. Furthermore, previous studies have indicated that the response of parenchymal cells to acetaminophen might be amplified by contributions from nonparenchymal cells such as liver sinusoidal endothelial cells and Kupffer cells (DeLeve et al., 1997; Ito et al., 2003; Holt et al., 2010). However, the toxicity observed in vitro monolayer culture models occurs much later than in vivo toxicity. With regard to these concerns, the liver tissue model includes several improvements that better mimic the in vivo situation. In fact, our results suggest that the response of hepatocytes to APAP toxicity was reinforced in IVL_{EHS}, probably via the maintenance of expression or up-regulation of cytochromes such as Cyp2e1. It is noteworthy that the activities of drug-metabolizing enzymes were higher in IVL_{EHS} than under other conditions (Fig. 5).

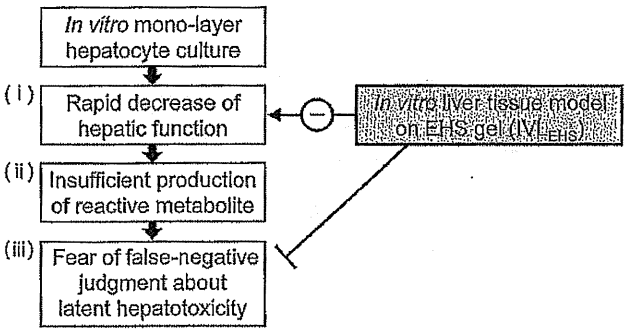

FIG. 6. Schematic illustration of the beneficial effect of IVL_{EHS} construction on both the responsiveness of hepatocytes and evaluation of hepatotoxicity.

So far, there have been no reports of the direct detection of NAPQI in hepatocytes, particularly in hepatocytes cultured on EHS gel. However, in this study, to confirm the functional metabolism of APAP in IVL_{EHS}, its cellular extract was assayed for mercapturate by CE-TOFMS (Table 3). This mercapturate form is produced metabolically from APAP via NAPQI (Soga et al., 2006). Because the NAPQI-dependent cytotoxicity is caused after the saturation of detoxification capability, intracellular administration of mercapturate suggests that IVL_{EHS} maintains a higher (or at least equivalent) metabolizing capacity than monocultures on EHS gel.

Conclusions

In summary, this study revealed the superiority of liver tissue models over the monolayer culture of hepatocytes. In short-term culture, EHS gel effectively maintained hepatic function; the further introduction of endothelial cells contributed to an early response to hepatotoxicant that mirrors the kinetics of the response in vivo. These results suggest that IVL_{EHS} is suitable for use as a compound-associated hepatotoxicity system and is superior to existing in vitro monolayer systems (Fig. 6). It is noteworthy that we performed the minimum modification necessary to archive the hepatic tissue-like structure. Many ingenious attempts have been made to mimic the in vivo liver architecture and developed improved systems for evaluating hepatotoxicity, e.g., micropatterning (El-Ali et al., 2006; Khetani and Bhatia, 2008), shear stress (Vinci et al., 2011), P450-inducers such as phenobarbital, and others. Incorporation of these technologies will contribute to the further improvement of our strategy.

Acknowledgments

We thank all members of our laboratory for their excellent animal care.

Authorship Contributions

Participated in research design: Toyoda and Tagawa.

Conducted experiments: Toyoda, Tamai, Kobayashi, Soga, and Tagawa.

Contributed new reagents or analytic tools: Kobayashi, Fujiyama, Soga, and Tagawa.

Performed data analysis: Toyoda, Tamai, and Kashikura.

Wrote or contributed to the writing of the manuscript: Toyoda and Tagawa.

References

Bhatia SN, Balis UJ, Yarmush ML, and Toner M (1998) Microfabrication of hepatocyte/fibroblast co-cultures: role of homotypic cell interactions. *Biotechnol Prog* **14**:378–387.

Bhatia SN, Balis UJ, Yarmush ML, and Toner M (1999) Effect of cell-cell interactions in preservation of cellular phenotype: cocultivation of hepatocytes and nonparenchymal cells. *FASEB J* **13**:1883–1900.

Bissell DM, Arenson DM, Maher JJ, and Roll FJ (1987) Support of cultured hepatocytes by a laminin-rich gel. Evidence for a functionally significant subendothelial matrix in normal rat liver. *J Clin Invest* **79**:801–812.

Dambach DM, Andrews BA, and Moulin F (2005) New technologies and screening strategies for hepatotoxicity: use of in vitro models. *Toxicol Pathol* **33**:17–26.

David JP (2005) The molecular toxicology of acetaminophen. *Drug Metab Rev* **37**:581–594.
DeLeve LD, Wang X, Kaplowitz N, Shulman HM, Bart JA, and van der Hoek A (1997) Sinusoidal endothelial cells as a target for acetaminophen toxicity. Direct action versus requirement for hepatocyte activation in different mouse strains. *Biochem Pharmacol* **53**: 1339–1345.
El-Ali J, Sorger PK, and Jensen KF (2006) Cells on chips. *Nature* **442**:403–411.
Gleeson MP, Hersey A, Montanari D, and Overington J (2011) Probing the links between in vitro potency, ADMET and physicochemical parameters. *Nat Rev Drug Discov* **10**:197–208.
Guillouzo A (1998) Liver cell models in in vitro toxicology. *Environ Health Perspect* **106** (Suppl 2):511–532.
Guillouzo A, Morel F, Fardel O, and Meunier B (1993) Use of human hepatocyte cultures for drug metabolism studies. *Toxicology* **82**:209–219.
Hayes MA and Pickering DB (1985) Comparative cytopathology of primary rat hepatocyte cultures exposed to aflatoxin B1, acetaminophen, and other hepatotoxins. *Toxicol Appl Pharmacol* **80**:345–356.
Hewitt NJ, Lechón MJ, Houston JB, Hallifax D, Brown HS, Maurel P, Kenna JG, Gustavsson L, Lohmann C, Skonberg C, et al. (2007) Primary hepatocytes: current understanding of the regulation of metabolic enzymes and transporter proteins, and pharmaceutical practice for the use of hepatocytes in metabolism, enzyme induction, transporter, clearance, and hepatotoxicity studies. *Drug Metab Rev* **39**:159–234.
Holt MP, Yin H, and Ju C (2010) Exacerbation of acetaminophen-induced disturbances of liver sinusoidal endothelial cells in the absence of Kupffer cells in mice. *Toxicol Lett* **194**:34–41.
Ito Y, Bethea NW, Abril ER, and McCuskey RS (2003) Early hepatic microvascular injury in response to acetaminophen toxicity. *Microcirculation* **10**:391–400.
Jaeschke H, Gores GJ, Cederbaum AI, Hinson JA, Pessayre D, and Lemasters JJ (2002) Mechanisms of hepatotoxicity. *Toxicol Sci* **65**:166–176.
Jaeschke H, Knight TR, and Bajt ML (2003) The role of oxidant stress and reactive nitrogen species in acetaminophen hepatotoxicity. *Toxicol Lett* **144**:279–288.
James LP, Mayeux PR, and Hinson JA (2003) Acetaminophen-induced hepatotoxicity. *Drug Metab Dispos* **31**:1499–1506.
Kaplowitz N (2005) Idiosyncratic drug hepatotoxicity. *Nat Rev Drug Discov* **4**:489–499.
Khetani SR and Bhatia SN (2008) Microscale culture of human liver cells for drug development. *Nat Biotechnol* **26**:120–126.
Kidambi S, Yarmush RS, Novik E, Chao P, Yarmush ML, and Nahmias Y (2009) Oxygen-mediated enhancement of primary hepatocyte metabolism, functional polarization, gene expression, and drug clearance. *Proc Natl Acad Sci USA* **106**:15714–15719.
Kikkawa R, Fujikawa M, Yamamoto T, Hamada Y, Yamada H, and Horii I (2006) In vivo hepatotoxicity study of rats in comparison with in vitro hepatotoxicity screening system. *J Toxicol Sci* **31**:23–34.
Kleinman HK and Martin GR (2005) Matrigel: basement membrane matrix with biological activity. *Semin Cancer Biol* **15**:378–386.
Kleinman HK, Philp D, and Hoffman MP (2003) Role of the extracellular matrix in morphogenesis. *Curr Opin Biotechnol* **14**:526–532.
Kola I and Landis J (2004) Can the pharmaceutical industry reduce attrition rates? *Nat Rev Drug Discov* **3**:711–715.
Kubota Y, Kleinman HK, Martin GR, and Lawley TJ (1988) Role of laminin and basement membrane in the morphological differentiation of human endothelial cells into capillary-like structures. *J Cell Biol* **107**:1589–1598.
Kwong E, Higgins J, and Templeton AC (2011) Strategies for bringing drug delivery tools into discovery. *Int J Pharm* **412**:1–7.
Lee SS, Buters JT, Pineau T, Fernandez-Salguero P, and Gonzalez FJ (1996) Role of CYP2E1 in the hepatotoxicity of acetaminophen. *J Biol Chem* **271**:12063–12067.
Matsumoto K, Yoshitomi H, Rossant J, and Zaret KS (2001) Liver organogenesis promoted by endothelial cells prior to vascular function. *Science* **294**:559–563.
Nahmias Y, Schwartz RE, Hu WS, Verfaillie CM, and Odde DJ (2006) Endothelium-mediated hepatocyte recruitment in the establishment of liver-like tissue in vitro. *Tissue Eng* **12**:1627–1638.
Ogawa S, Tagawa Y, Kamiyoshi A, Suzuki A, Nakayama J, Hashikura Y, and Miyagawa S (2005) Crucial roles of mesodermal cell lineages in a murine embryonic stem cell-derived in vitro liver organogenesis system. *Stem Cells* **23**:903–913.
Paul SM, Mytelka DS, Dunwiddie CT, Persinger CC, Munos BH, Lindborg SR, and Schacht AL (2010) How to improve R&D productivity: the pharmaceutical industry's grand challenge. *Nat Rev Drug Discov* **9**:203–214.
Reid AB, Kurten RC, McCullough SS, Brock RW, and Hinson JA (2005) Mechanisms of acetaminophen-induced hepatotoxicity: role of oxidative stress and mitochondrial permeability transition in freshly isolated mouse hepatocytes. *J Pharmacol Exp Ther* **312**:509–516.
Schmidt C, Bladt F, Goedecke S, Brinkmann V, Zschiesche W, Sharpe M, Gherardi E, and Birchmeier C (1995) Scatter factor/hepatocyte growth factor is essential for liver development. *Nature* **373**:699–702.
Seglen PO (1976) Preparation of isolated rat liver cells. *Methods Cell Biol* **13**:29–83.
Soga T, Baran R, Suematsu M, Ueno Y, Ikeda S, Sakurakawa T, Kakazu Y, Ishikawa T, Robert M, Nishioka T, et al. (2006) Differential metabolomics reveals ophthalmic acid as an oxidative stress biomarker indicating hepatic glutathione consumption. *J Biol Chem* **281**:16768–16776.
Soga T, Igarashi K, Ito C, Mizobuchi K, Zimmermann HP, and Tomita M (2009) Metabolomic profiling of anionic metabolites by capillary electrophoresis mass spectrometry. *Anal Chem* **81**:6165–6174.
Soto-Gutierrez A, Navarro-Alvarez N, Yagi H, Nahmias Y, Yarmush ML, and Kobayashi N (2010) Engineering of an hepatic organoid to develop liver assist devices. *Cell Transplant* **19**:815–822.
Strain AJ (1999) Ex vivo liver cell morphogenesis: one step nearer to the bioartificial liver? *Hepatology* **29**:288–290.
Takashi H, Katsumi M, and Toshihiro A (2007) Hepatocytes maintain their function on basement membrane formed by epithelial cells. *Biochem Biophys Res Commun* **359**:151–156.
Tsuisui M, Ogawa S, Inada Y, Tomioka E, Kamiyoshi A, Tanaka S, Kishida T, Nishiyama M, Murakami M, Kuroda J, et al. (2006) Characterization of cytochrome P450 expression in murine embryonic stem cell-derived hepatic tissue system. *Drug Metab Dispos* **34**:696–701.
Vinci B, Duret C, Klieber S, Gerbal-Chaloin S, Sa-Cunha A, Laporte S, Suc B, Maurel P, Ahluwalia A, and Daujat-Chavanieu M (2011) Modular bioreactor for primary human hepatocyte culture: medium flow stimulates expression and activity of detoxification genes. *Biotechnol J* **6**:554–564.

Address correspondence to: Yoh-ichi Tagawa, Associate Professor, Department of Biomolecular Engineering, Graduate School of Bioscience and Biotechnology, Tokyo Institute of Technology, 4259-B-51 Nagatsuta-cho, Midori-ku, Yokohama 226-8501, Japan. E-mail: ytagawa@bio.titech.ac.jp

Bioinformatics Tools for Mass Spectroscopy-Based Metabolomic Data Processing and Analysis

Masahiro Sugimoto[1,2,3,*], Masato Kawakami[1,4], Martin Robert[1,2], Tomoyoshi Soga[1,4] and Masaru Tomita[1,4]

[1]*Institute for Advanced Biosciences, Keio University, Tsuruoka, Yamagata 997-0017, Japan*

[2]*Systems Biology Program, Graduate School of Media and Governance, Keio University, Fujisawa, Kanagawa 252-8520, Japan*

[3]*Graduate School of Medicine and Faculty of Medicine Kyoto University, Yoshida-Konoe-cho, Sakyo-ku, Kyoto 606-8501, Japan*

[4]*Department of Environment and Information Studies, Keio University, Fujisawa, Kanagawa 252-8520, Japan*

Abstract: Biological systems are increasingly being studied in a holistic manner, using *omics* approaches, to provide quantitative and qualitative descriptions of the diverse collection of cellular components. Among the *omics* approaches, metabolomics, which deals with the quantitative global profiling of small molecules or metabolites, is being used extensively to explore the dynamic response of living systems, such as organelles, cells, tissues, organs and whole organisms, under diverse physiological and pathological conditions. This technology is now used routinely in a number of applications, including basic and clinical research, agriculture, microbiology, food science, nutrition, pharmaceutical research, environmental science and the development of biofuels. Of the multiple analytical platforms available to perform such analyses, nuclear magnetic resonance and mass spectrometry have come to dominate, owing to the high resolution and large datasets that can be generated with these techniques. The large multidimensional datasets that result from such studies must be processed and analyzed to render this data meaningful. Thus, bioinformatics tools are essential for the efficient processing of huge datasets, the characterization of the detected signals, and to align multiple datasets and their features. This paper provides a state-of-the-art overview of the data processing tools available, and reviews a collection of recent reports on the topic. Data conversion, pre-processing, alignment, normalization and statistical analysis are introduced, with their advantages and disadvantages, and comparisons are made to guide the reader.

Keywords: Bioinformatics, mass spectrometry, metabolome, metabolomics, software development, statistical analysis, systems biology.

1. INTRODUCTION

Metabolomics or metabolome analysis aims to conduct the simultaneous determination and quantitative analysis of intracellular metabolites. Since metabolomics is concerned with small molecules that are the substrates and products, of cellular activity, it allows to explore in a direct and immediate way the biological system/environment interface. This can be appreciated by the great sensitivity of metabolite levels to subtle pharmacological and toxicological intervention [1-6]. As a consequence, metabolomics is playing an increasingly important role in systems biology, a field that aims to integrate information collected at multiple biological levels. It is now used widely in many applications including microbiology, diagnostic biomarker discovery, toxicological testing, food and beverage analysis, plant and animal phenotyping, and drug discovery and development [7-12].

Nuclear magnetic resonance (NMR) is one of the most commonly used analytical techniques in metabolomics studies [13]. To date, a number of large-scale, studies using NMR have been reported, including blood urine and serum metabolome profiling [14-15]. This technique has been popular in metabolomic studies because of its quantitative nature and high reproducibility. In addition, NMR spectra provide a wealth of biochemical information not available by other means [16-20]. It also has definitive advantage that it can be used in non-destructive ways to enable metabolomic profiling *in vivo* [21-22] and even allow metabolite imaging in biological samples [23-24]. However, the relatively low sensitivity of NMR, and the spectral overlap that often occurs, limits the number and variety of metabolites that can be simultaneously observed. Hyphenated mass spectrometry (MS) methods, such as GC-MS [25], LC-MS [26] and CE-MS [27], currently provide higher sensitivity, and are the leading analytical platform for metabolite profiling [28-31]. Because of the diverse physical and chemical properties (for example, molecular weight, polarity and solubility) of the metabolites contained in typical samples, no single analytical methodology can profile datasets comprehensively. Thus, metabolomics, in the strictest sense, is very challenging, and the term is used broadly to cover approaches concerned with investigating subsets of the metabolome [32]. GC-MS, LC-MS and CE-MS are generally capable of profiling volatile, singly or multiply charged metabolites. Hyphenated

*Address correspondence to this author at the Institute for Advanced Biosciences, Keio University, Tsuruoka, Yamagata 997-0052, Japan;
Tel: +81-235-25-0528; Fax: +81-235-25-0574;
E-mail: msugi@sfc.keio.ac.jp

2212-392X/12 $58.00+.00

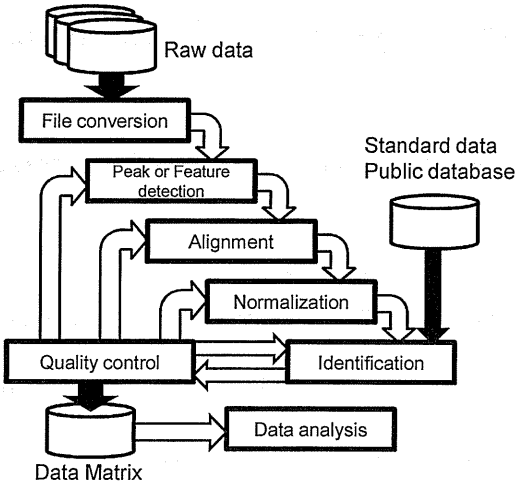

Fig. (1). Typical processing flow of MS data in the field of metabolomics. Raw data are sequentially processed in multiple phases, including file conversion, feature detection, alignment and normalization. Standard data and public databases that include metabolite information, such as mass spectrometric data, are used for subsequent feature identification. These processes are then assessed using quality control criteria and the previous phase is repeated if necessary. Once calibrated, the data matrix (aligned detected features across multiple datasets) can be transferred for subsequent data analysis phases.

MS methods involve the use of a physico-chemical separation method in tandem with a mass spectrometer, which is used for detection. These systems thus produce data that is multidimensional with a time and mass/charge ratio component. The multidimensionality of the data increases the data processing challenges posed by metabolomics.

Because metabolomics deals with large datasets like other *omics*, sophisticated computational tools are vital for efficient and high-throughput analysis, to eliminate systematic bias and to explore biologically significant findings. In this paper, we review bioinformatics topics in the field of metabolomics, with an emphasis on hyphenated-MS methods, especially LC-MS and CE-MS. As some of these topics have been well reviewed previously [33-51], we emphasize the most recent innovations and developments in the field. In the first part, we review the main data processing steps, including data formats/conversion, feature extraction/detection, comparison of multiple datasets including migration time and mass spectral alignment, signal normalization and identification of metabolites, and quality control (QC). The second part focuses on downstream data analysis of processed datasets, using univariate or multivariate statistical analyses, classification and clustering. We also discuss the standardization of data format, compare some of the leading software tools that implement different algorithms for data processing and discuss data interpretation for different research applications.

2. DATA PROCESSING FOR METABOLOMICS ANALYSIS

Typical data processing flow for MS data has been previously reviewed by Katajamaa and Orešič [34], and is now implemented in a variety of software packages [52-57]. The analytical usually flow starts from data conversion, detecting signal peaks, normalization and comparison of multiple datasets to generate a data matrix that includes the detected peaks of all given samples (alignment). The differentiation of signals from noise by interpretation of the mass spectrum and the identification of detected features using, for example, alignments with standard compound data, are also important. Finally, processed data are analyzed using statistical methods and data mining. A recent addition to this straightforward analytical process is the quality control (QC) of data processing. This process does not simply involve the use of QC methods after data processing [58], but rather is used as part of an iterative feedback loop between data processing and QC [59] (Fig. **1**).

The following section introduces recent literature related to 1) data conversion, 2) feature detection, 3) alignment, 4) scaling/normalization, 5) identification, and 6) QC. See also the following references: [58, 60-61].

2.1. Data Conversion

Data processing starts with file format conversion from the MS-vendor dependent binary format to more common formats, to allow subsequent processing to be carried out on independent operation systems and software. A common and open framework and data description is important if data are to be shared among laboratories [62-64]. NetCDF and mzXML are the most commonly used file formats to store hyphenated-MS data [65]. Owing to recent rapid improvements in the throughput and resolution of MS, individual data files have become large, which compounds problems associated with the large numbers of datasets handled in metabolomics projects. Although these common file formats simplify data sharing between laboratories, the problem of handling a large number of large datasets remains. While removing small intensity peaks and data compression using irreversible filtering, as can be implemented in mzMine [56] and mzMine2 [52], is the simplest way to diminish data size, they risk distorting subsequent data analysis. Although Mass++ allows the direct import of various binary files provided by MS venders into standard software [66], it merely accesses the binary data through a vendor-provided application programmable interface (API). This dramatically reduces throughput and does not solve the problem of MS-vendor software dependency. Although it cannot be shown directly without access to the source code, most vendor-provided hyphenated-MS instrument binary formats (for example, wiff files and .D formats provided by Applied Biosystems and Agilent Technologies Inc.) can be estimated to contain a series of mass spectra data, since mass spectra are usually collected in this way. This data structure results in much longer data access times to output a chromatograph or an electropherogram if the data points included in the mass spectra are not unique over the chromatograph or electropherogram. To solve these size and structure problems, we developed a compact binary file format that facilitates rapid access to chromatographs or electropherograms and mass spectra [67]. Although there is currently a trade-off between facilitating quick data access and the availability of a generic file format, the development and standardization of file formats that fulfill the requirement for rapid access should be a priority.

2.2. Feature Detection

In the typical analytical flow, three-dimensional data incorporating retention or migration times, *m/z* and intensity data are first converted to piles of two-dimensional chromatography/electropherograms, by integrating data points within a specific range along the *m/z* axis (ion extraction or data binning). Second, background reduction (or baseline removal) and smoothing of the data are conducted to reduce false positive detection. Third, local maxima are found as peak top candidates, or a mathematical model is fitted to find peak-like shapes within the chromatographs or electropherograms. These are used to identify peaks over a user-specified threshold, which may be in the form of a peak height, peak area or signal-to-noise (S/N) ratio [52-54, 67-68]. Although wavelet transformation and Gaussian-curve fitting (or matched filter) is a commonly used means to distinguish signal from noise [53, 68], fully automatic processing remains difficult owing to the complex peak shapes often observed in LC-MS and, in particular, CE-MS. Interactive tuning of the algorithms is therefore often required [52, 67]. Other options are to identify peaks at matched locations (*m/z* and time), even under the initially-defined threshold after the alignment process [69]. Such feedback procedures and QC will be discussed further in section 2.7.

2.3. Alignment of Multiple Data Sets

The alignment of multiple datasets, i.e. the elimination of retention or migration times shifts between datasets, is a central topic of data processing in the metabolomics field, and is associated with specific technical difficulties. Therefore, many alignment techniques have been developed [70]. The retention time variance of GC-MS and LC-MS datasets is non-linear [71], and thus multiple sophisticated time correction methods have been developed. The alignment of CE-MS data is especially difficult because of the low reproducibility of migration times [54], and robust and versatile alignment procedures are therefore required. Here, we review the three major alignment algorithms used for the temporal dimension. In addition, the normalization of mass/charge ratio (*m/z*) calculated by MS is also introduced.

Time Correlation Optimized Warping

Time correlation optimized warping (COW) divides chromatograms into small segments and shifts individual segments to maximize the correlation coefficient between a reference and test chromatograph. The algorithm itself has inherent problems; a larger number of segments leads to greater accuracy, but raises the risk of dividing the targeted metabolite peaks. To optimize the degree of segmentation, the use of heuristic and global optimization processes, such as genetic algorithms, has been proposed [72]. To date, benchmark tests with only small numbers of peaks have been performed [72], and the method should be evaluated using data with a large number of peaks, observed by high resolution MS.

Parametric Time Warping

The parametric time warping method aligns a given chromatogram with a reference chromatogram using second degree polynomial functions, called warping functions [73]. Coefficients in warping functions are optimized to minimize the time difference between selected matched peaks in reference and aligned chromatograms. Thus, the method relies on the presence of a number of known matched peaks among the samples to be aligned. Although the addition of internal standards (IS) is the most simple way to achieve this, it has several disadvantages: (i) suitable IS compounds must be carefully selected, for example the IS compounds must not normally be present in the samples; (ii) additional sample preparation is required; and most significantly (iii) the added IS may cause ion suppression effects and degrade the quantitative reliability of the observed profiles. Despite these problems, rapid computation time is an important advantage of this method. Lower flexibility and accuracy has been reported for this method in comparison with COW and dynamic time warping (DTW) [70].

Dynamic Time Warping

DTW finds the matched peaks among multiple datasets automatically to produce warping functions. Dynamic programming (DP) has historically been used in homology searching of genes or genomes, and has been used for matching peaks [74]. The parameters that characterize DP results, such as gap penalty, make this method parametric. Thus, empirical reiterative multi-step optimization of these parameters has been used in CE-MS data processing software [54] and interactive graphical user interfacing [67]. In contrast, recent modifications to DTW using multiple chromatograms with different *m/z*, instead of one-dimensional information available from total ion chromatography, reduced the impact of the parametric problems embedded in the original DTW algorithm [75].

Calibration of Mass Values (m/z Alignment)

Exact masses (mass-to-charge ratio (*m/z*) values), produced by detectors in time-of-flight (TOF)-MS instruments are usually calculated based on online calibration with one or more reference substances that are co-injected with the sample. This is known as the mass lock system [76]. The *m/z* values detected for individual peaks fluctuate depending on several factors, including temperature, the abundance of ions simultaneously entering the MS, and the processing ability, type and specifications of the MS detector [77]. Thus, the data acquired should be further calibrated. Typically a calibration curve generated using the peaks of known *m/z* is applied to correct *m/z* values of other peaks of interest (offline or software calibration) [78-80]. The *m/z* values are intricately calibrated for the whole chromatograph or electropherogram time axis, since the factors influencing *m/z* shifts can change even during the course of a single run [81]. In addition, *m/z* value correction can be carried out using peak intensities relative to the intensities of internal standards [82], using the location of background noise observed throughout the measurement [83], and using statistical approaches with multiple datasets [69]. Ideally, these methods should be integrated to optimize *m/z* normalization.

2.4. Scaling and Normalization

The elimination of unwanted systematic bias, while maintaining genuine biological differences in the observed datasets, is essential for subsequent analyses to identify significant metabolites. The systematic bias derived from

variation in sample concentration, especially when handling biofluids such as urine, blood and saliva samples, must be removed. Deviation in signal intensities due to measurement errors, for example poor MS sensitivity, must also be removed. To address the former problem, metabolomic analyses typically use endogenous metabolites, for example creatinine, to normalize overall urine metabolite concentrations [84]. However, this method is not always sufficient to eliminate systematic bias, and a recent mouse metabolomic study revealed a correlation between overall urinary metabolites and several physical parameters, such as age and weight [85]. The latter bias is generally removed using two approaches. Despite the increased technical complexity of sample preparation, the use of internal standard compounds added to the sample before or after extraction is the most common approach. The use of multiple internal standards to normalize closely eluting peaks with similar *m/z* values has also been reported [86]. Otherwise, normalization methods based on several statistical models (unit norm [87] median [88] and quantile [58]), scaling methods (auto scaling, range scaling, Pareto scaling, vast scaling and level scaling) [61], and data transformation (log and power) have been widely used. These methods are, however, inferior to the internal standard-based methods [58].

2.5. Identification of Metabolites

Global metabolic profiles or fingerprints that do not necessarily assign observed features to particular metabolites can be very powerful means of classifying and directly comparing samples. They highlight metabolomics as providing a global molecular signature allowing us to discriminate groups of samples in contrast to more conventional comparisons based on single metabolite. However, metabolite identification from spectral data remains indispensable for providing mechanistic insight into specific cellular or disease processes and in quality control/assurance industry, for example. The accurate identification of a compound usually requires the ability to match candidate spectra with standard compounds run under the same conditions. Matching to either externally or internally applied standards has been commonly used, the latter making use of isotopically labeled standards or samples. However, the lack of readily available standard compounds remains a major obstacle to confirming the identity of observed compounds. The purification of compounds from complex samples allows access to standards; however, this can be an expensive and time-consuming process. Several tools that estimate compound composition using isotope distribution or fragmentation patterns in the mass spectrum have been developed [89-92]. Databases that include a large number candidate compounds are also indispensable (see review [43]). A theoretical study estimated that the mass spectral information available from mass spectrometers with accuracy approaching 1 ppm, such as TOFMS, is not sufficient to identify peaks without a matched standard compound, as multiple candidate compounds are often retrieved from the large public databases [93]. The Human Metabolome Project has already identified more than 4,000 putative endogenous metabolites from human serum using GC-MS, LC-MS and NMR profiles with computer-aided literature mining [12]. Many studies thus use tandem MS, which generates more informative spectra including many fragment peaks, for compound identification [94-95]. Efforts have also been made to use retention time information to reduce the number of possible candidates. These efforts are based on reverse engineering techniques [96-99] or theoretical simulation [100], which predict the retention/migration times from the metabolite structure. The quantification of observed peaks in the absence of matched standard compounds is also difficult, but computational prediction techniques have been developed [101]. The combined use of such computational methods can greatly reduce the number of candidates and aid metabolite identification.

2.6. Quality Control of Data Processing

A number of algorithms have been developed for data processing, especially for peak detection and alignment, and various parameters can be used to characterize the quality of data processing [59]. The selection of the best algorithm, and the best parameters, to analyze the datasets obtained is not an easy task. Thus, QC evaluation based on various benchmark tests is important to understand the features of each algorithm and their parameters [102].

A comparison of peak detection algorithms of LC-MS data using centWave [68], matched filter implemented in XCMS [53] and MZmine [56] showed that there was only a partial overlap in the results obtained with these methods, and a number of peaks were only detected by one software (not overlapped) [68]. Even with the same algorithm, the use of different parameters strongly affected peak detection performance [58]. Evaluation of the alignment of LC-MS data using six freely available software packages, including XCMS [53], MZmine [56], msInspect [103] and OpenMS [55], concluded that no single software perfectly aligned the datasets [104]. The annotation of metabolite identities using fixed confidence thresholds has been recommended for data reporting, as has quantitative assessment of the annotation quality using the false discovery rate (FDR) [105]. Another approach is to provide a sophisticated graphical interface that enables specific steps of data processing to be rerun using different parameters [52]. Scripting tools may also be used to accelerate the optimization process and to minimize the need for user interactivity. Another possible means to improve performance entails the development of an iterative analytical framework with machine learning methods that allow the program to be trained to tune parameters using the difference between automated and manual data processing [59]. It is evident that subsequent statistical analysis will benefit if care is taken at the processing stage, and that automatic data processing for peak detection, alignment and annotation remain far from perfect.

3. DATA ANALYSIS IN METABOLOMICS

Once a data matrix has been produced from raw data, subsequent steps usually involve different forms of statistical analysis and data mining to allow the identification of samples or variables (metabolites) that capture the bulk of variation between datasets and that may represent candidates for biologically meaningful variables. Typical analyses of metabolomic data consist of two phases; initially an overview of the given datasets is generated using

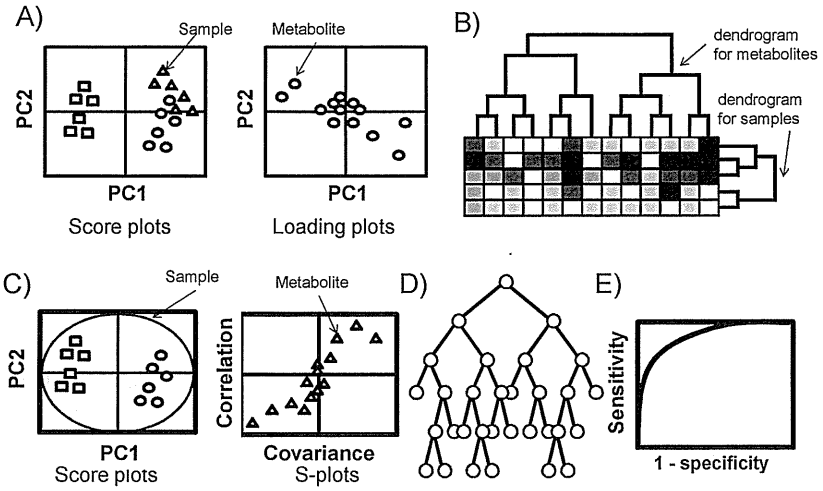

Fig. (2). Typical data analysis methods used in the field of metabolomics. Score plots in PCA **A**), dendrograms of clustering **B**), score plots and S-plots of PLS-DA **C**), random forests model **D**), and ROC curve **E**).

multivariate analysis and individual peaks are subsequently graded by univariable analysis. Here we briefly introduce several univariable and multivariate analyses, and classification and assessment methods that are widely used in analyzing MS-based metabolomics datasets (Fig. **2**). Selected recent applications are then introduced. See also the recent reviews [37, 43].

3.1. Principal Component Analysis

Principal component analysis (PCA) is an unsupervised statistical analysis that is probably the most widely used statistical tool in metabolomics studies. PCA converts high-dimensional data into fewer dimensions, by projecting the data into a reduced dimensional subspace, while maintaining as much variance from the original data as possible [106-108]. The procedure is repeated until the datasets can be presented usually within two or three dimensions. This facilitates visual inspection of the distributed samples in principal component (PC) space, using score plots [33]. The Euclidian distance between individual samples in score plots reflects the degree of systematic variation in metabolite profiles among samples, and loading plots show the contribution of individual metabolites to each PC (Fig. **2A**). Prior to the development of more effective data analyses, such as clustering, pattern recognition or classifications, the vast majority of metabolomic studies used PCA as a first exploratory step [37].

3.2. Cluster Analysis

Clustering analysis is a statistical method that involves dividing observed datasets into several subclasses or clusters based on a selected statistical distance function. There are two types of clustering algorithms: hierarchical and non-hierarchical methods. Both algorithms partition the observed datasets into subgroups so that datasets with similar metabolomic profiles are placed in each subgroup [33]. Hierarchical clustering (HCL) (Fig. **2A**) aligns datasets by generating dendrograms using the following procedure: 1) calculate the similarity of the two samples using a specific metric, such as Pearson correlation, Euclidean, mutual information and covariance values; 2) align the most similar samples as neighbors or pair them as a single cluster; and 3) reiterate step 1 and 2 until all samples are aligned [33]. Non-hierarchical clustering (non-HCL) also divides data into clusters but without any hierarchical organization. The K-means and fuzzy c-means methods are typical examples of non-HCL [33]. In the K-means method, k data points are initially randomly chosen to be close to the mean of each cluster, a new mean is then calculated for each cluster and the patterns are reassigned to the new means. This process is repeated until the cluster means are such that no pattern moves from one cluster to another [109]. The K-means method assigns each datapoint into only one cluster while the fuzzy c-means method allows data to be assigned to multiple clusters [110]. Fuzzy c-means also calculates the probability of a datapoint belonging to each cluster [111]. These analyses are widely used when the number of clusters for the samples is unknown, and can be used for one-time snapshot profiling as well as time-course data.

3.3. Partial Least Squares Analysis

Partial least squares (PLS) (Fig. **2C**), a regression-based method, builds a low-dimensional sub-space based on linear combinations of the original X variables. It makes use of additional Y information by adjusting the model to capture the (Y)-related variation into the original X variables [37]. PLS is particularly useful when fewer observations (samples) are available than measured variables (metabolites). In metabolomics, PLS-based classification and PLS-discriminant analysis (PLS-DA) have been widely used to sharpen the separation between groups or observations. This is achieved by rotating PCs to maximize the separation between known classes, and to elucidate the variables that carry the class separating information [33,112-113]. Similarly to loading plots in PCA, S-plots visualize both the covariance and the correlation between metabolites and the modeled class designation. The S-plot therefore helps to identify statistically significant and potentially biochemically significant metabolites, based both on contributions to the model and their reliability [114]. Despite its powerful ability to separate classes, care must be taken during fitting of PLS-DA to the training detaining datasets, which exaggerate

generalization ability. Usually cross-validation or permutation tests are used to assess the ability of the trained PLS-DA model [115]. Orthogonal projections to latent structures (OPLS)-DA, an extension of PLS-DA featuring an integrated orthogonal signal correction filter to remove variability not relevant to class separation, has been used increasingly owing to its robustness against noise [21,116].

3.4. Random Forests

Random forests (RF) is a relatively new machine learning method typically used to discriminate two groups (Fig. **2D**). The fundamental concept of RF is to allow data structures to be understood without dimensional reduction, and this method is therefore different from conventional methods such as PCA and PLS-DA. This classification algorithm was developed by Leo Breiman [117] and uses an ensemble of classification trees. Each of the classification trees is built using a bootstrap sample of the data, and at each split, the candidate set of variables is a random subset of the variables. Thus, RF uses both bagging (bootstrap aggregation), a successful approach for combining unstable learners, and random variable selection for tree building. Each tree is unpruned (grown fully) so as to obtain low-bias trees. At the same time, bagging and random variable selection result in low correlation of the individual trees [118]. The algorithm yields an ensemble that can achieve both low bias and low variance (by averaging over a large ensemble of low-bias, high-variance but low-correlation trees) [119].

3.5. Conventional Statistical Analysis

Because metabolomics generates data on multiple (dozens or hundreds) different metabolites, global overview methods that take into account the possible correlations between variables are the main tools used. However, when used appropriately, monovariate methods can also provide useful insight and remain widely used, especially for secondary biomarker analyses.

Although multivariate classification methods are often used to identify biomarkers, the discrimination of individual metabolites is usually assessed by conventional univariate statistical tests, such as Student's t-test and the Mann-Whitney test for two classes, or ANOVA and Kruskal-Wallis for multiple classes (≥3). Dependency or correlations between metabolites, inadequate sample size, and large FDR due to multiple hypothesis testing must be taken into account when applying these methods [120]. Corrections of the *p*-value and/or calculation of false discovery rates must be carried out to limit the number of false positives that increase linearly with the number of variables [120]. Multivariate analysis has the advantage of considering the general patterns in the whole dataset, but it introduces additional challenges and sources of variability owing to the necessary data pre-treatment and scaling used to analyze all variables at once [61]. Thus, biomarkers should be rigorously evaluated by a combination of these statistical analyses and several validation methods, such as cross-validation and bootstrap analysis [121]. Recently, the FDR and receiver operating characteristics (ROC) methods have been frequently used to identify significantly different metabolites in the given classes.

The FDR method [122], is commonly used in gene expression analyses, and is now also used in metabolomic studies, [11], where a large number of variables are analyzed simultaneously, and thus multiple comparisons are conducted. In practice, FDR establishes a threshold for the significance level (*q*-value) that can be expected to represent false positives among all significant hypotheses to reject optimistic significance. To account for multiple comparisons, each FDR is estimated by the product of the significance level (Type I error rate) and the number of null hypotheses tested, divided by the number of null hypotheses rejected [123].

A ROC [124] curve is a statistical representation that simultaneously expresses both sensitivity and specificity to separate binary class datasets, for example to discriminate healthy control and patient datasets. The curve is plotted by fractions of sensitivity as the Y-axis vs. fractions of false positive rate (1- specificity) as the X-axis (Fig. (**2E**)). The test is used to differentiate performance of one or a combination of biomarkers; an area under the curve (AUC) of 1.0 indicates perfect separation without any false negatives or false positives, while an AUC of 0.5 is equivalent to random separation only.

AUC evaluates only the rank of the metabolites associated with the given classes, and therefore it does not count fold-change or the concentration itself. Meanwhile, FDR evaluates the relative significance of the metabolites in a large group of metabolites. Thus, the use of a combination of different methods, along with multivariate analyses, can achieve more efficient screening than any single method.

3.6. Data Mining Analysis

In addition to classification methods, other data mining methods have also been used in metabolomic data analyses to discriminate two classes, for example support vector machine (SVM) [125-126], artificial neural networks (ANN) [127] and decision tree [128]. ANN has been particularly widely used for various applications in MS-based studies, including in metabolite identification [97], classification [129], optimization of separation parameters [130] and QC of data processing [59] (see review [131]). In comparative study, a class of LC/MS peaks was predicted by four data mining techniques, k-NN, SVM, PLS-DA and Naïve Bayes, and revealed that the former two methods performed better than the latter two [132]. However, it is usually difficult to select the best method for the analysis of a given metabolomic dataset *a priori*, and the development of a pipeline with multiple analytical tools is therefore necessary. Visualization of metabolomic data in a pathway form also requires several data mining techniques. Small relevance and conditioned metabolic pathways have been predicted and then merged to generate pruned networks [133]. Small sub-pathways were estimated with only relevant nodes, for example metabolite and enzymes, to reduce complexity and to enhance interpretability [134]. Both of these method attempts to find new relevant connections, rather than to assign the observed data to known maps.

4. VISUALIZATION AND DATA SHARING

Here we discuss data visualization to facilitate the interpretation of large metabolomic profiles. Data

standardization is also discussed to realize open and shared access to metabolomics technologies.

4.1. Visualization of Metabolomics Data

Data visualization using a heatmap or a pathway form facilitates comprehension of the metabolomic change/response to the experimental setting. MetaboAnalyst visualizes experimental metabolomic data using heatmap visualization and offers common statistical analyses, such as PCA, PLS-DA, and HCL [135-136]. Pathway Project [137] visualizes data in the form of several graph types, such as bar graphs, time-courses and simple circles corresponding to metabolite concentration at the metabolite node on the KEGG pathway [138]. Similar web-based network visualization tools for BioCyc [139] are also available [140]. Both tools take advantage of Google Map API zoom and search functions, which can be helpful when looking for interesting details in large metabolomic datasets. The editable pathway tool is also useful when new molecular interactions that are not available in public database are to be explored [141].

4.2. Standardization of Metabolomics Data Reporting

In addition to the standardization of raw file format and data processing tools, the standardization of the reporting of metabolomic data information has also received attention. This would facilitate experimental replication, interrogation and comparison over multiple investigators and laboratories. The Metabolomics Society has formed five working groups, biological context metadata, chemical analysis, data processing, ontology and data exchange, to establish guidelines for reporting standards [142]. The Chemical Analysis Working Group, part of the Metabolomics Standards Initiative, proposed a set of minimum information that should be provided when reporting chemical analyses, and these included metadata from MS and NMR data, sample processing protocol, data processing, metabolite identification, and even unknown metabolites in the obtained dataset [143]. Attempts to define standards for data reporting have been made but unfortunately are still not widely used [35, 142-143]. To maximize the value of metabolomic datasets, it is important that data is made publicly available in formats, and with metadata, that are widely accepted as standard. In this sense, the field of metabolomics lags behind genomics and proteomics. Some of the reasons for this slow adoption of standards include the heterogeneity of analytical platforms and vendors, and the complexity of sample processing, which remains the focus of ongoing investigation. A Metabolomics Standard Initiative was recently initiated by the Metabolomics Society, and aims to develop standards for data exchange, ontology and guidelines for data reporting to solve some of the current issues (http://msi-workgroups.sourceforge.net/).

5. SOFTWARE TOOLS

A number of free software packages are already available for the processing and analysis of metabolomic data, and Table **1** gives a sample directory of these. Both web services and desktop applications are available. The table is not necessarily exhaustive, but should help to identify commonly used solutions. Several statistical tools listed were designed for NMR data analyses but might be also useful for MS data analyses. Here, we focused only on tools used specifically in metabolomics studies, and did not review free or commercial generic software for multivariate analysis or other standard statistical analysis. We emphasize mainly tools for pre-processing and data visualization. Moreover, details of these packages are not reviewed here, and the reader is referred to the original publication or project web site for more information.

6. APPLICATIONS

Here, the use of statistical methods in several applications is discussed. Note that several of the statistical analysis applications introduced here used NMR data. The same multivariable techniques can technically be used for MS data analyses, but it should be noted that MS-data includes a larger number of variables (metabolites) and therefore more redundant variables. However, appropriate statistical analyses and MS data may provide more powerful insight into biological context.

PCA and PLS-DA have been the most popular and widely used analyses in metabolomic studies. Although PCA can visualize the similarities and differences in the observed data with unknown classes, it is generally used as a weaker classification tool for class known problems. It is therefore generally used as a first screening method for classification problems, prior to PLS-DA. For example, while PCA was able to give adequate separation resolution of various conditions, for example smokers and non-smokers in a salivary metabolite profile, PLS-DA was subsequently used to maximize resolution [144]. A similar approach was adopted for the discrimination of lung cancer sufferers using urine metabolomic profiles [116] and pancreatic cancer using serum metabolomic profiles [145]. HCL has also been used to assess data structure by aligning datasets based on their profile's similarities [146-148], and this method is often used to classify samples with known classes, similarly to PCA. It has been applied to biomarker discovery, to classify control and patient groups, with key branches in its dendrogram indicating biomarker candidates [149]. Although this example was not a metabolomics application, a particularly successful example of HCL involved the clustering of gene expression in breast cancer, which suggested the existence of a new subtype of breast cancer in addition to the known classes [150]. The assessment of the analytical results of these methods can only be performed with known classes, and new findings should be analyzed further once consistency between results and known classes has been confirmed.

The over-fitting of a developed model to a given dataset should be carefully avoided, especially when using MS data, since it usually involves a large number of variables and small sample numbers. RF is expected to be a useful classification method when we use such datasets. Because the algorithm itself does not limit the application, RF has been used for biomarker discovery in urine metabolomic profiles from breast cancer patients [125] and in plant applications to explore genotype-dependent variables in metabolomic profiles in *Arabidopsis* and potato [151-152]. When RF and margin-based classifiers, such as SVM and PLS-DA, were compared, RF and SVM were found to have similar accuracy and both were slightly better than PLS-DA

Table 1. Software List for Metabolomic Analysis

Name	Main Application	Specific Features	Ref.	License	User Interface
OpenMS	Raw data processing	C++ libraries for MS data processing, including feature detection and protein/peptide identification	[57]	Lesser GNU Public License (LGPL)	C++ library
CDK-Taverna	Workflow	A workflow based data processing library for cheminformatics	[156]	LGPL	Plug-in of Java
Metabonomic Package	Statistical analysis of NMR data	Multivariate analysis, such as PCA, PLS, k-nearest neighbor classification, neural networks.	[127]	GPL	R language*)
metaXCMS	Importing XCMS output	Post processing of XCMS for comparison of multiple (≥3) classes and visualizing statistical analyses.	[157]	Free	R language*) and GTK
XCMS	Processing LC-MS raw data	R module for data processing, including feature detection and peak alignment	[53]	Free	R language*)
XCMS2	Importing tandem mass spectrometry (MS/MS) raw data	Processing of tandem mass spectrometry data for metabolite identification and structural characterization	[158]	Free	Plug-in of R language*)
MeDDL	Data processing of LC-MS and GC/MS data	A Matlab script for data processing and visualizing multiple datasets.	[159]	Free	Matlab script
MetaScape	Pathway visualization / statistical analysis	A Cytoscape plug-in for visualizing and interpreting metabolomic data in the context of human metabolic networks	[160]	Free	Plug-in of Cytoscape
MetaboliteDetector	Importing NetCDF and FastFlight GC-MS data	Comprehensive analysis, including chromatogram compression, feature detection, alignment and compound identification.	[161]	GNU public license (GPL)	Local application (GUI)
MetAlign	Importing many common formats, including Masslynx, Xcalibur, netCDF, and the old-style HP/Agilent format of GC-MS / LC-MS data	Interface-driven data processing program. Includes baseline correction, smoothing, feature detection and alignment	[162]	Free	Local application (GUI)
MAVEN	Data processing of LC-MS and pathway visualization	Tools for all aspects of data analysis, from feature extraction to pathway-based graphical data display	[59]	Free	Local application (GUI)
LIMSA	Data processing / mass spectrometric lipidome data	Tool finds and integrates peaks in a mass spectrum and matches the peaks with a user-supplied list of expected lipids.	[163]	Free	Local application (GUI)
centWave	Data processing of LC-MS data	Detection of close and partially overlapping features; also has the highest overall recall	[68]	Free	Local application (GUI)
mzMine2	Data processing of MS data	Modular framework for processing, visualizing and analyzing mass spectrometry-based molecular profile data	[52]	Free	Local application (GUI)
JDAMP	Data processing of CE-MS data	Data processing, alignment, differential display	[67]	Free for academic users	Local application (GUI)
CytoScape	Pathway visualization / statistical analysis	Software for the visualization and analysis of biological networks	[164]	Free	Local application (GUI)
metaP-server	Statistical analysis, database searching, pathway visualization	A web-based metabolomics data analysis tool	[165]	Free	Web
MetDAT	Statistical analysis, database searching, pathway visualization	A modular and workflow-based free online pipeline for mass spectrometry data processing, analysis and interpretation	[166]	Free	Web
ChromaA	Alignment, chromatography-mass spectrometry	Signal-based retention time alignment for chromatography-mass spectrometry data	[167]	Free	Web
MZedDB	Data processing	Interactive *m/z* annotation tool	[92]	Free	Web
Pathway projector	Pathway visualization	A Web-based zoomable pathway browser that uses KEGG atlas and Google Maps API	[137]	Free	Web
MetPA	Pathway visualization / statistical analysis	A web-based metabolomics tool for pathway analysis and visualization	[168]	Free	Web
MetExplore	Pathway visualization	A web server to link metabolomic experiments and genome-scale metabolic networks	[169]	Free	Web

Table 1. cont...

MSEA	Pathway visualization	A web-based tool to identify biologically meaningful patterns in quantitative metabolomic data	[170]	Free	Web
MetabolomeExpress	Pipeline for data processing and statistical analysis of GC/MS data	Data processing, statistical analysis (e.g. HCL), metabolite identification and heat map visualization	[171]	Free access for non-commercial and academic users	Web
Chromaligner	Alignment of LC-MS data	Alignment of LC-MS chromatographs using the COW algorithm	[172]	Free access	Web

*) R language (http://www.r-project.org/).

[125]. However, the accuracy of the model trained on the given dataset is not the only important factor. Validation, which involves confirming the generalizability of the model's accuracy and the significance of selected variables in similar experiments, is important when such discriminate models are used. SVM and PLS-DA can also be used to rank the significance of variables constitutive to the models, while RF does not explicitly maximize the margin, which makes the trained model unbiased to the given datasets and is directly related to the generalizability [151]. Although several techniques to evaluate generalizability are known, including the permutation test, bootstrap test and cross-validation [115], rigorous assessment has indicated that normal cross-validation is insufficient and overfitting may remain a problem [153]. Thus, careful and multilateral evaluation of the developed model is necessary.

After multivariate analysis, individual metabolites or sets of metabolites are usually accessed using univariate analyses. As ROC is a conventional statistical method that has been widely used for medical diagnosis problems, it has become popular in biomarker discovery applications. Multiple logistical regression models, composed of multiple metabolite markers to discriminate liver diseases [154] and oral cancers [155], were assessed using AUC values calculated from ROC. This revealed the discrimination possible when only a few metabolite sets are used, rather than all available data, which is used in PCA and PLS-DA. Approaches using all available metabolites are appropriate when studying overall variation, but are not useful for clinical usage, for example in the development of diagnosis techniques using a single or a few markers. Thus, integrative analyses using multivariate analysis, feature selection, and assessment of individual or a few markers are standard techniques that are useful for general purposes.

As should be apparent, multiple solutions exist for data processing, some of which are capable of performing most or all steps from raw data to statistical analysis, while others are specialized for certain steps or visualization. The selection of a data analysis solution is not straightforward and will depend on the analytical platform, the experimental design and data type, and on computational infrastructure, among other things. This review gives an overview of the options that can be chosen from, and highlights recent efforts to integrate these solutions to generate simple, yet powerful methods for the user. The field of data analysis for metabolomics is still rapidly evolving, and ongoing efforts are likely to produce further progress. There is a need for greater interchangeability and interoperability between tools, and unfortunately the profusion of new and interesting tools originating from numerous small groups often tends to limit this goal. Developers should consider these factors when promoting particular solutions. This will stimulate data sharing and exchange, and therefore improve adoption by a community of users who are often overwhelmed by a range of possibilities, and who may therefore tend to stick to tools that emphasize usability rather than quality or performance.

In this review article, we reviewed multiple tools for processing and analysis of MS data. Multiple metabolomics platforms together with the appropriate data processing and analysis tools can allow us to identify discriminating features in a set of samples, with multiple applications in research, diagnosis, etc. However, beyond class discrimination, understanding the biological mechanisms responsible for the variance in observed profiles remains an important issue. For this, the constant development and improvement of computational techniques for metabolite identification, accurate quantification, data integration, and pathway visualization is important and will continue to be the focus of bioinformatics efforts in the coming years.

CONCLUSION

Remarkable improvements in analytical instruments, including MS, have enabled the profiling of metabolites with increasingly high throughput and high precision. Bioinformatics, which facilitates the interpretation of the output of these instruments, is essential to the successful analysis of large dataset metabolomic applications. Tool development must keep up with the improvements in analytical instruments and thus represents an important challenge, but has great potential to add value to metabolomic datasets.

CONFLICT OF INTEREST

Declared none.

ACKNOWLEDGEMENTS

This work was supported by research funds from the Yamagata Prefectural Government and the City of Tsuruoka. We thank Akira Oikawa at the Riken Plant Science Center and Fumio Matsuta at Kobe University for fruitful discussions.

REFERENCES

[1] Lindon JC, Holmes E, Nicholson JK. Metabonomics in pharmaceutical R&D. FEBS J 2007; 274: 1140-51.

[2] Swann J, Wang Y, Abecia L, *et al.* Gut microbiome modulates the toxicity of hydrazine: a metabonomic study. Mol Biosyst 2009; 5:

351-5.

[3] Fonville JM, Maher AD, Coen M, Holmes E, Lindon JC, Nicholson JK. Evaluation of full-resolution J-resolved 1H NMR projections of biofluids for metabonomics information retrieval and biomarker identification. Anal Chem 2010; 82: 1811-21.

[4] Nicholson JK, Wilson ID, Lindon JC. Pharmacometabonomics as an effector for personalized medicine. Pharmacogenomics 2011; 12: 103-11.

[5] Nicholson JK, Wilson ID. Opinion: understanding 'global' systems biology: metabonomics and the continuum of metabolism. Nat Rev Drug Discov 2003; 2: 668-76.

[6] Lindon JC, Holmes E, Nicholson JK. So what's the deal with metabonomics? Anal Chem 2003; 75: 384A-91A.

[7] Gieger C, Geistlinger L, Altmaier E, *et al.* Genetics meets metabolomics: a genome-wide association study of metabolite profiles in human serum. PLoS Genet 2008; 4: e1000282.

[8] Ishii N, Nakahigashi K, Baba T, *et al.* Multiple high-throughput analyses monitor the response of E. coli to perturbations. Science 2007; 316: 593-7.

[9] Fiehn O, Kopka J, Dörmann P, Altmann T, Trethewey RN, Willmitzer L. Metabolite profiling for plant functional genomics. Nat Biotechnol 2000; 18: 1157-61.

[10] Hirayama A, Kami K, Sugimoto M, *et al.* Quantitative metabolome profiling of colon and stomach cancer microenvironment by capillary electrophoresis time-of-flight mass spectrometry. Cancer Res 2009; 69: 4918-25.

[11] Sreekumar A, Poisson LM, Rajendiran TM, *et al.* Metabolomic profiles delineate potential role for sarcosine in prostate cancer progression. Nature 2009; 457: 910-4.

[12] Psychogios N, Hau DD, Peng J, *et al.* The human serum metabolome. PLoS One 2011; 6: e16957.

[13] Reo NV. NMR-based metabolomics. Drug Chem Toxicol 2002; 25: 375-82.

[14] Holmes E, Loo RL, Stamler J, *et al.* Human metabolic phenotype diversity and its association with diet and blood pressure. Nature 2008; 453: 396-400.

[15] Vlaanderen J, Moore LE, Smith MT, *et al.* Application of OMICS technologies in occupational and environmental health research; current status and projections. Occup Environ Med 2010; 67: 136-43.

[16] Van QN, Issaq HJ, Jiang Q, *et al.* Comparison of 1D and 2D NMR spectroscopy for metabolic profiling. J Proteome Res 2008; 7: 630-9.

[17] Rothman DL, Novotny EJ, Shulman GI, *et al.* 1H-[13C] NMR measurements of [4-13C]glutamate turnover in human brain. Proc Natl Acad Sci U S A 1992; 89: 9603-6.

[18] Weiss RG, Chacko VP, Glickson JD, Gerstenblith G. Comparative 13C and 31P NMR assessment of altered metabolism during graded reductions in coronary flow in intact rat hearts. Proc Natl Acad Sci U S A 1989; 86: 6426-30.

[19] Artemov D, Pilatus U, Chu S, Mori N, Nelson JB, Bhujwalla ZM. Dynamics of prostate cancer cell invasion studied in vitro by NMR microscopy. Magn Reson Med 1999; 42: 277-82.

[20] Bothwell JH, Griffin JL. An introduction to biological nuclear magnetic resonance spectroscopy. Biol Rev Camb Philos Soc 2011; 86: 493-510.

[21] Weljie AM, Bondareva A, Zang P, Jirik FR. (1)H NMR metabolomics identification of markers of hypoxia-induced metabolic shifts in a breast cancer model system. J Biomol NMR 2011; 49: 185-93.

[22] Keun HC, Athersuch TJ. Nuclear magnetic resonance (NMR)-based metabolomics. Methods Mol Biol 2011; 708: 321-34.

[23] Wu CL, Jordan KW, Ratai EM, *et al.* Metabolomic imaging for human prostate cancer detection. Sci Transl Med 2010; 2: 16ra8.

[24] Ma LH, Li Y, Djurić PM, Maletić-Savatić M. Systems biology approach to imaging of neural stem cells. Methods Mol Biol 2011; 711: 421-34.

[25] Fiehn O, Kopka J, Trethewey RN, Willmitzer L. Identification of uncommon plant metabolites based on calculation of elemental compositions using gas chromatography and quadrupole mass spectrometry. Anal Chem 2000; 72: 3573-80.

[26] Plumb R, Granger J, Stumpf C, Wilson ID, Evans JA, Lenz EM. Metabonomic analysis of mouse urine by liquid-chromatography-time of flight mass spectrometry (LC-TOFMS): detection of strain, diurnal and gender differences. Analyst 2003; 128: 819-23.

[27] Soga T, Ohashi Y, Ueno Y, Naraoka H, Tomita M, Nishioka T. Quantitative metabolome analysis using capillary electrophoresis mass spectrometry. J Proteome Res 2003; 2: 488-94.

[28] Aharoni A, Ric de Vos CH, Verhoeven HA, *et al.* Nontargeted metabolome analysis by use of Fourier Transform Ion Cyclotron Mass Spectrometry. OMICS 2002; 6: 217-34.

[29] Castrillo JI, Hayes A, Mohammed S, Gaskell SJ, Oliver SG. An optimized protocol for metabolome analysis in yeast using direct infusion electrospray mass spectrometry. Phytochemistry 2003; 62: 929-37.

[30] Theodoridis G, Gika HG, Wilson ID. Mass spectrometry-based holistic analytical approaches for metabolite profiling in systems biology studies. Mass Spectrom Rev 2011; 30: 884-906

[31] Bajad S, Shulaev V. LC-MS-based metabolomics. Methods Mol Biol 2011; 708: 213-28.

[32] Monton MR, Soga T. Metabolome analysis by capillary electrophoresis-mass spectrometry. J Chromatogr A 2007; 1168: 237-46.

[33] Blekherman G, Laubenbacher R, Cortes DF, *et al.* Bioinformatics tools for cancer metabolomics. Metabolomics 2011; 7: 329-343

[34] Katajamaa M, Orešič M. Data processing for mass spectrometry-based metabolomics. J Chromatogr A 2007; 1158: 318-28.

[35] Arita M. What can metabolomics learn from genomics and proteomics? Curr Opin Biotechnol 2009; 20: 610-5.

[36] Holmes C, McDonald F, Jones M, Ozdemir V, Graham JE. Standardization and omics science: technical and social dimensions are inseparable and demand symmetrical study. OMICS 2010; 14: 327-32.

[37] Boccard J, Veuthey JL, Rudaz S. Knowledge discovery in metabolomics: an overview of MS data handling. J Sep Sci 2010; 33: 290-304.

[38] Saito K, Matsuda F. Metabolomics for functional genomics, systems biology, and biotechnology. Annu Rev Plant Biol 2010; 61: 463-89.

[39] Scalbert A, Brennan L, Fiehn O, *et al.* Mass-spectrometry-based metabolomics: limitations and recommendations for future progress with particular focus on nutrition research. Metabolomics 2009; 5: 435-58.

[40] Dunn WB, Broadhurst DI, Atherton HJ, Goodacre R, Griffin JL. Systems level studies of mammalian metabolomes: the roles of mass spectrometry and nuclear magnetic resonance spectroscopy. Chem Soc Rev 2011; 40: 387-426.

[41] Yetukuri L, Ekroos K, Vidal-Puig A, Oresic M. Informatics and computational strategies for the study of lipids. Mol Biosyst 2008; 4: 121-7.

[42] Sumner LW, Urbanczyk-Wochniak E, Broeckling CD. Metabolomics data analysis, visualization, and integration. Methods Mol Biol 2007; 406: 409-36.

[43] Tohge T, Fernie AR. Web-based resources for mass-spectrometry-based metabolomics: a user's guide. Phytochemistry 2009; 70: 450-6.

[44] Barbas C, Moraes EP, Villaseñor A. Capillary electrophoresis as a metabolomics tool for non-targeted fingerprinting of biological samples. J Pharm Biomed Anal 2011; 55: 823-31.

[45] Mamas M, Dunn WB, Neyses L, Goodacre R. The role of metabolites and metabolomics in clinically applicable biomarkers of disease. Arch Toxicol 2011; 85: 5-17.

[46] Dunn WB. Current trends and future requirements for the mass spectrometric investigation of microbial, mammalian and plant metabolomes. Phys Biol 2008; 5: 011001.

[47] Ramautar R, Mayboroda OA, Somsen GW, de Jong GJ. CE-MS for metabolomics: Developments and applications in the period 2008-2010. Electrophoresis 2011; 32: 52-65.

[48] Ramautar R, Somsen GW, de Jong GJ. CE-MS in metabolomics. Electrophoresis 2009; 30: 276-91.

[49] Britz-McKibbin P. Capillary electrophoresis-electrospray ionization-mass spectrometry (CE-ESI-MS)-based metabolomics. Methods Mol Biol 2011; 708: 229-46.

[50] Bowen BP, Northen TR. Dealing with the unknown: metabolomics and metabolite atlases. J Am Soc Mass Spectrom 2010; 21: 1471-6.

[51] Baena B, Cifuentes A, Barbas C. Analysis of carboxylic acids in biological fluids by capillary electrophoresis. Electrophoresis 2005; 26: 2622-36.

[52] Pluskal T, Castillo S, Villar-Briones A, Oresic M. MZmine 2: modular framework for processing, visualizing, and analyzing mass spectrometry-based molecular profile data. BMC Bioinformatics 2010; 11: 395.